

Bond characterization between concrete base and repairing SFRC by pull-off tests

Everaldo Bonaldo
Joaquim O. Barros, Paulo B. Lourenço

Report 04-DEC/E-13

*The present research has been carried out under the financial
support of FCT, under PhD grant number SFRH / BD / 11232 / 2002*

Date: May 2004

No. of pages: 57

Keywords: pull-off test, epoxy adhesive, thin-bonded overlay, steel fibre reinforced
concrete



Escola de
Engenharia



Departamento de
Engenharia Civil



Universidade
do Minho



Contents

Summary	3
1 Introduction	4
Background	4
Objective and Scope	6
2 Materials	7
Concrete Substrate and Concrete Overlay	7
Bond Products	9
3 Test Set-up	11
Preparation of the Specimens	11
Pull-Off Test Method and Equipment	13
4 Results	18
Tests Performed Manually with Proceq DYNA Z15	18
Assessing the Influence of Loading Rate	27
5 Summary and Conclusions	29
Acknowledgements	31
References	32
ANNEXES	34
Annex A - Physical properties of the aggregates	35
Annex B - Particle sizing of the aggregates	37
Annex C - Data of the compressive strength of the substrate concrete and of the SFRC overlay	40
Annex D - Bond coat dosage adopted and respective proportions	42
Annex E - Failure surface recorded	43
Annex F - Data of the tests for two controlled stress rates	55



Summary

In the last years an emerging repair and strengthening technique for concrete slabs has been used, consisting of applying a thin layer of steel fibre reinforced concrete (SFRC) onto the existent concrete slab. The performance of the structural system depends on the bonding behaviour between old and new concretes. Adhesives based on epoxy resins currently make this liaison. The prices of these adhesives are quite different depending, mainly, on the percentage of pure resin that they include. In the present report, three commercial adhesive compounds of distinct prices and properties were selected to bond concrete base and repairing SFRC. The bond behaviour was assessed from pull-off tests and the influence of the strength class of concrete base and repairing SFRC was analysed. Finally, the performance of the adhesives was evaluated, considering both the bond strength and their prices.



1 Introduction

Background

Thin overlays repair made of cementitious materials, resinous materials and polymer-modified cementitious materials are being used for strengthening and rehabilitation purposes in concrete pavements, concrete bridges and asphalt pavements (KNAB, 1988; AUSTIN et al., 1995; VAYSBURD and McDONALD, 1999; DELATTE and SEHDEV, 2003). Due to the enhanced properties of steel fibre reinforced concrete (SFRC), such as ductility under compression and high flexural toughness, it is expected that SFRC is advantageous in those applications.

The present work deals specifically with the bond between SFRC overlay and concrete substrate, and is a part of a more comprehensive work, which aims at evaluating the structural performance of thin bonded SFRC in the strengthening and rehabilitation of laminar structures.

The development and maintenance of a sound bond between the overlay and the existing concrete substrate is an essential requirement for the performance of the strengthening purpose. If sufficient adhesion is achieved, it enables the structure to behave monolithically in resisting loading and curling stresses (AUSTIN et al., 1995; VAYSBURD and McDONALD, 1999; DELATTE and SEHDEV, 2003).

The pull-off test method is one of the tensile test methods commonly used to assess the adhesion between the repair overlay and the existing concrete substrate. In this test method, the tensile stress between old and new concrete is maximum.

According to the ASTM D4541 standard (1995), the general pull-off test is performed by securing a loading fixture (disc) normal (perpendicular) to the surface of the coating, fixed with an adhesive. After the adhesive harden, a testing apparatus is attached to the loading fixture and aligned, in order to apply a tensile force normal to the surface to be tested. The force applied to the loading fixture is then gradually increased in a manner as smooth and continuous as possible, using a specified loading rate. Failure occurs along the weakest plan within the system comprised of the test fixture, adhesive, repair overlay, bond surface between overlay and substrate, and substrate.

Unlike the other bond test methods, whose use is restricted to laboratorial fracture, the pull-off test can be easily used in the field evaluation of the bond strength between repair material and parent concrete in a structure. A notable limitation of this type of test is its relative poor precision, evidenced by the large variation values obtained with different types of apparatus. As pull-off strength measurements depend on instrumental parameters, results obtained using different devices may not be comparable (VAYSBURD and McDONALD, 1999; ASTM D4541, 1995).

There are essentially four different modes of failure for pull-off tests of a concrete patch repair. Failures can occur at the base concrete, at the bond interface, at the overlay, at the epoxy used to bond the disc to the core. A combination of these failures can also occur. These different failure modes provide valuable information about the overlay system. The magnitude and location of the fracture surface gives some information of the performance of the repair system (overlay and adhesive). When failure only mobilizes adhesion material the strength provides a true indication of the bond strength. In this case, the ultimate load is a direct measure of the adhesion between the overlay and the concrete substrate. Failures at other locations indicate that the bond strength is greater than the tensile strength of the base concrete and concrete overlay. When failure occurs between the disk and the overlay surface, there is an adhesive failure. In this case, if the result is lower than the average of the others results it should be discarded, otherwise it can be taken into account. An epoxy failure should be a rare occurrence. If the failure occurs in the overlay material, the repair material is the weakest part of the system. In this case the bond strength exceeds the applied ultimate stress. This is referred as a cohesive failure of the overlay. Finally, if the fracture surface occurs in the substrate, or in the underlying concrete, the overlay (repair) concrete and the adhesive layer are stronger than the existing concrete, and the repair can be considered adjusted. This is again often referred as a cohesive failure of the substrate. In this case, the pull-off stress is the tensile strength of the concrete substrate. In some cases the failure occurs partially along the bond surface and partially in either the overlay or concrete substrate, and the fracture surface is a combination of two or more of the failures modes aforementioned (SPRINKEL and OZYILDIRIM, 2000; FHA, 2000).

According to SPRINKEL and OZYILDIRIM (2000), for practical purposes, failures at the base concrete or at overlay provide an indication of the degree to which the overlay is anchored and are considered as indicating bond strength. For these authors, when a failure occurs in the epoxy, the result should be discarded if it is lower than the average of the other results, or included if it is of the same or higher level. **Table 01** shows a range of bond strength to qualify the test results.

Table 01 - Bond strength qualification (SPRINKEL and OZYILDIRIM, 2000).

Bond strength (MPa)	Label
≥ 2.1	excellent
1.7 to 2.1	very good
1.4 to 1.7	good
0.7 to 1.4	fair
0 to 0.7	poor

Objective and Scope

The present study has the following objectives:

- Investigate the effect of the substrate and the overlay resistance on the adhesion strength;
- Evaluate the bond performance of three commercially available bond products for bonding purpose.

The experimental program is composed by three main series, each one with a distinct concrete strength class for the substrate. Each of this series is composed by two series of two different concrete strength classes for the overlay, resulting a total of six series, as indicated in **Table 02**.

The following classes of concrete substrate were considered: low class (C20/30), medium class (C40/50), usually achieved in practice, and high class (C60/70). For the concrete overlay, a variety of strength classes were used: from low class (C20/30), up to high class (C65/75). The concrete overlay was always reinforced with steel fibres.

A maximum difference of one strength class was adopted in each series in order to minimize a tendency of the failure mode at the lower strength class material.

Table 02 - Concrete classes of the tests.

Concrete substrate (ordinary concrete)	Concrete overlay (with steel fibres)
C16/20	C20/25 C30/37
C35/45	C35/45 C45/55
C55/67	C55/67 C60/75

2 Materials

The following sections detail the various materials used in the present work.

Concrete Substrate and Concrete Overlay

A laboratory trial phase was developed at the Laboratory of the Structural Division of the University of Minho aiming to establish three compressive strength grades for the concrete base, according to CEB-FIP Model Code (1993): C16/20, C35/45, C55/67; and six compressive strength grades for the concrete layer reinforced with steel fibres (SFRC): C20/25, C25/30, C35/45, C45/55, C55/67 and C60/75.

For the purpose of defining the mix properties, a Faury mix design method was used, see e.g. COUTINHO (1988), together with aggregates available in the Northern Region of Portugal (Minho). Details about the physical properties of the aggregates are provided in **Annex A**. In **Annex B** the sieve analyses of the aggregates and the information about maximum aggregate size are included. Hooked ends DRAMIX[®] RC-80/60-BN steel fibres were used to reinforce the concrete overlay. This fibre has a length (l_f) of 60 mm, a diameter (d_f) of 0.75 mm, an aspect-ratio (l_f / d_f) of 80 and a yield strength of about 1100 MPa (DRAMIX, 1998). In previous work it was verified that this fibre has high performance since significant increase in the ultimate load bearing capacity of the structural concrete elements was obtained (BARROS & FIGUEIRAS, 1998).

Table 03, 04 and **05** show the mix proportion applied, as well as, the main properties of the ordinary concrete (substrate) and SFRC overlay. Here, the percentage of superplasticizer refers to the weight of cement plus fly ash, W/C is the water-cement ratio, W/(C+FA) is the water- binder (cement plus fly ash) ratio. The superplasticizer adopted was RHEOBUILD 1000. **Table 04** refers to mix proportions of overlay concrete used for bond coat applied on dry substrate surface. **Table 05** refers to mix proportions for bond coat applied on saturated substrate. More details regarding the compressive strength of the adopted concretes mixes can be found in **Annex C**.

Table 03 - Mix proportions and main properties of the ordinary concrete.

Components	Designation		
	B1 (C16/20)	B2 (C35/45)	B3 (C55/67)
Cement I 42.5 R (kg/m ³)	225	300	425
Fine river sand (kg/m ³)	356	353	337
Coarse river sand (kg/m ³)	597	591	564
Fine aggregate 4/11 (kg/m ³)	444	439	419
Coarse aggregate 11/16 (kg/m ³)	566	560	535
Superplasticizer (%)	2.5	2.5	2.5
W/C ratio	0.68	0.45	0.30
Slump (mm)	60	225	250
f _{C28d} ^(*) (MPa)	22.32	42.59	60.82

^(*) Average value of 3 cylinder specimens (150 mm x 300 mm)

Table 04 - Mix proportions and main properties of the steel fibre-reinforced concrete (bond coat applied on dry substrate surface).

Components	Designation					
	C1 (C20/25)	C2 (C25/30)	C3 (C35/45)	C4 (C45/55)	C5 (C55/67)	C6 (C60/75)
Cement I 42.5 R (kg/m ³)	220	290	290	360	400	460
Fly Ash (kg/m ³)	22	29	29	36	40	46
Fine river sand (kg/m ³)	349	339	339	328	322	306
Coarse river sand (kg/m ³)	584	567	567	549	540	512
Fine Aggregate 4/11 (kg/m ³)	434	422	422	408	401	381
Coarse aggregate 11/16 (kg/m ³)	554	538	538	521	512	486
Superplasticizer (%)	2.5	2.5	2.5	2.5	2.5	2.5
Steel fibre (kg/m ³)	30	30	30	30	30	30
W/(C+FA) ratio	0.65	0.48	0.48	0.37	0.32	0.31
Slump ⁽⁺⁾ (mm)	110	200	180	210	220	250
f _{C28d} ^(*) (MPa)	25.87	32.08	41.50	53.51	62.54	66.81

⁽⁺⁾ slump before adding the steel fibres

^(*) Average value of 3 cylinder specimens (150 mm x 300 mm)

Table 05 - Mix proportions and main properties of the steel fibre-reinforced concrete (bond coat applied on saturated substrate surface).

Components	Designation				
	C1' (C20/25)	C2' (C30/37)	C3' (C50/60)	C4' (C55/67)	C5' (C60/75)
Cement I 42.5 R (kg/m ³)	220	280	290	400	475
Fly Ash (kg/m ³)	22	28	29	40	48
Fine river sand (kg/m ³)	347	329	339	322	315
Coarse river sand (kg/m ³)	581	552	567	540	528
Fine Aggregate 4/11 (kg/m ³)	432	410	422	401	393
Coarse aggregate 11/16 (kg/m ³)	551	523	538	512	501
Superplasticizer (%)	2.5	2.5	2.5	2.5	2.5
Steel fibre (kg/m ³)	30	30	30	30	30
W/(C+FA) ratio	0.67	0.57	0.48	0.34	0.25
Slump ⁽⁺⁾ (mm)	170	245	230	225	275
f _c ^(*) (MPa)	27.36 (55)	38.48 (52)	58.46 (49)	64.34 (49)	63.10 (44)

⁽⁺⁾ slump before adding the steel fibres

^(*) Average value of 3 cylinder specimens (150 mm x 300m)
(value) age at testing

Bond Products

Epoxy resin is widely used as the bond product for most materials used in construction, such as concrete, masonry units, wood, glass, and metals. Epoxy resin is also a good adhesive to bond fresh to hardened concrete. Bonding fresh concrete overlay to an existing slab is an example of such application (ACI 503R-93).

Three types of epoxy-based bond agents were selected to bond fresh SFRC overlay to hardened concrete substrate, namely two epoxy resin-based products (P1 and P2), and one epoxy resin and cement-based product (P3). **Table 06** and **07** show some summarized information about the bond products.

The bond P1 and P2 coating materials were applied onto dry and clean, i.e., free from surface contaminants such as dust, laitance, oil or grease, following the manufacturer specifications.

To evaluate the influence of the surface conditions on the bond coat material, P3 was applied onto two types of substrate surface: dry surface and saturated surface. In **Annex D** the dosages adopted and proportions for each component are included.

Table 06 - Data extracted from commercial datasheet for the bond products (SIKA, 2002).

Product	Commercial name	Dosage	Brief description
P1	Icosit® K 101	0.5 to 2 kg/m ² , depending on porosity and roughness of the substrate surface.	Epoxy resin-base bond coat, free from solvents, available in two components. Ensures the perfect bond between freshly concrete and old concrete.
P2	Sikadur® 32 N	0.3 to 0.8 kg/m ² , depending on nature and porosity and also temperature.	Epoxy resins-base bond coat available in two components, free from solvents. When applied on the hardened concrete surface provides perfect bond between freshly and old concrete.
P3	Sikatop® Armatec 110 EpoCem®	When used as adhesion agent, at least, 1.5 kg/m ² , can be higher if the concrete substrate is very irregular.	Anticorrosive coating and adhesive agent cement and modified epoxy resin-base, available in three components.

Table 07 - Physical properties of the products extracted from commercial datasheet (SIKA, 2002).

Product	Properties		
	Specific gravity	Bond strength	Mechanical resistance
P1	Approximated 1.8 kg/l	to concrete: ~3 MPa (concrete failure) to sandblasted steel: ~20 MPa	Compressive strength: ~90 MPa Flexural strength: ~45 MPa
P2	Approximated 1.4 kg/l	to concrete: 2.5 - 3.0 MPa (concrete failure) to steel: 18 - 20 MPa	Compressive strength: ~60 - 70 MPa Tensile strength: ~18 - 20 MPa Flexural strength: ~30 - 35 MPa
P3	Approximated (at 20°C) A+B+C mix 2.0 kg/l	to sandblasted concrete: 2 - 3 MPa to steel: 1 - 2 MPa	-

3 Test Set-up

Preparation of the Specimens

Nonreinforced concrete slabs of 300 mm x 650 mm, with 80 mm thickness, were used as concrete substrate. All substrate slabs were cast at different periods. For each batch of concrete three cylindrical concrete specimens, measuring 150 mm in diameter and 300 mm long, were cast.

After the slabs and the cylindrical concrete specimens have been cast, burlap sacks were placed over the slabs. The burlap sacks were monitored and kept wet for two days. Following the initial curing procedures, the slabs and the cylindrical specimens were demoulded and maintained in normal laboratory conditions for 28 days after have been cast.

When the concrete substrate attained 28 days of age, the top surface (casting surface) of the slab specimen was treated. The bond product was then applied and the freshly concrete overlay was cast. The work of bonding the plastic SFRC overlay to the hardened concrete followed the manufactures specifications (SIKA, 2002) and the ACI guidelines (ACI 503.2-92, ACI 503.5R-92 and ACI 503.6R-97). For the aims of this research, an overlay thickness of approximately 30 mm of SFRC layer was adopted.

Likewise for substrate concrete, three cylindrical concrete specimens (150mm x 300mm) for each batch of SFRC were cast and tested on the 28th day. The aforementioned curing process was also adopted for the thin SFRC overlay and cylindrical concrete specimens.

Figure 01 shows a specimen before surface treatment and the equipment used to rough the surface. The process of roughing the top surface of the concrete substrate has the purpose of removing a very thin layer of the surface, in order to remove grease, oils, free particles, laitance or dirt, as well as producing an irregular surface. **Figure 02** shows the main bond steps. When the concrete overlay attained an age of about 28 days, the partial core was drilled and the pull-off tests were carried out.



Figure 01 - The specimen surface before roughing (a) and the rough machine (b).

It is stressed that a mini slipform paver (**Figure 02 (g)**) was used to consolidate the SFRC overlay. The mini slipform intends to simulate the real conditions of compaction of a thin SFRC overlay (**Figure 03**).

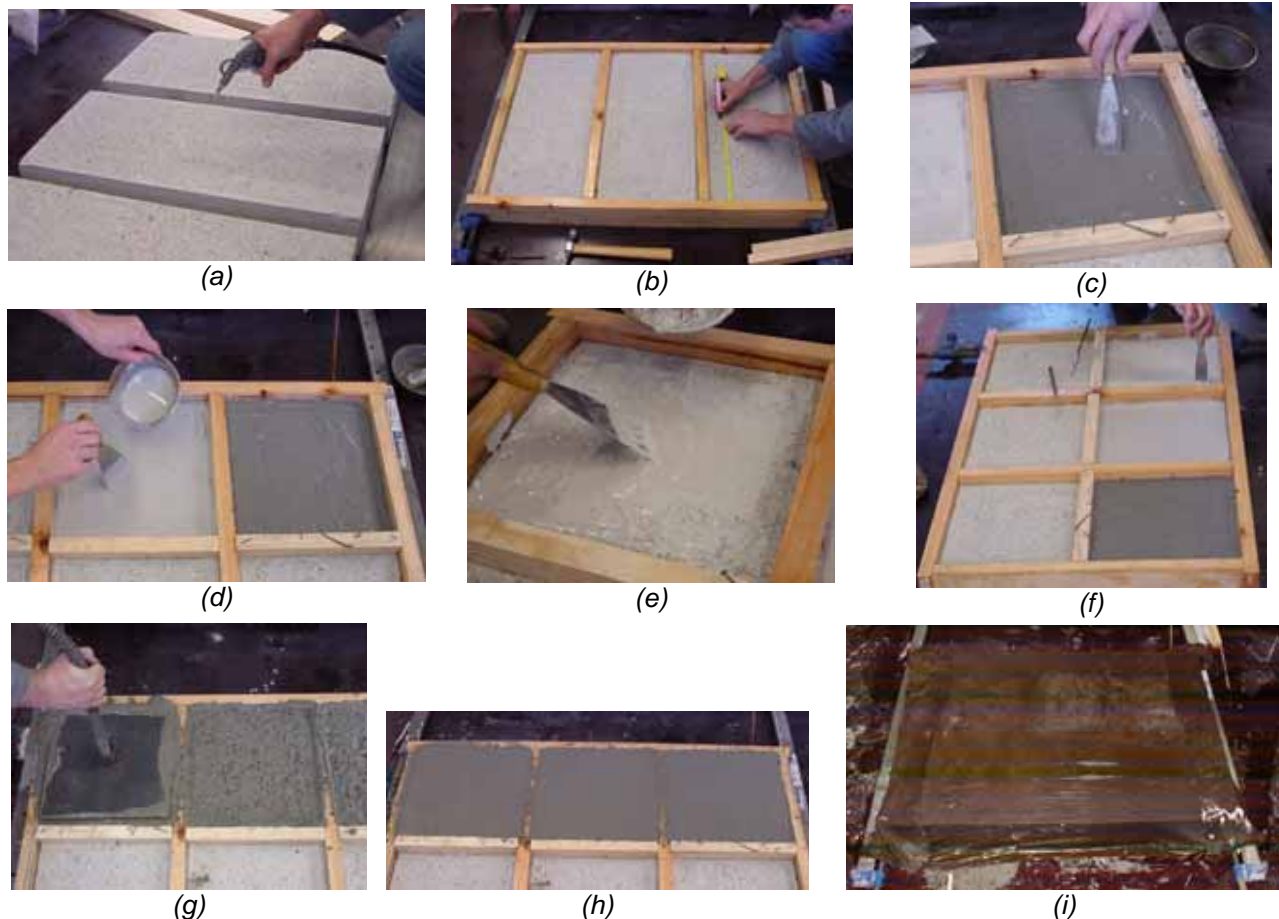


Figure 02 - Main steps of the bond process of the SFRC overlay: (a) cleaning the top surface with compressed air jet, (b) definition of the area for each bond coat material, (c) placing the bond product P3, (d) placing the bond product P2, (e) placing the bond product P1, (f) overview of the bond coats before casting the freshly laid SFRC overlay, (g) consolidating of the SFRC, (h) final aspect of the finished surface, (i) curing with wet burlap.



Figure 03 - Roller screed (revolving tube) for fixed-form paving on a street.
[Photo: www.pavement.com]

Pull-Off Test Method and Equipment

When compared to other tests, the pull-off test is simpler and popular tensile bond test (**Figure 04**) for measuring the adhesion properties, both on site for quality control and, in the laboratory, to evaluate the materials properties and failure modes (AUSTIN et al., 1995; VAYSBURD and McDONALD, 1999; CHMIELEWASKA et al., 2003). There are many factors affecting the results of the method. Regarding this issue, CHMIELEWASKA et al (2003) presented a statistical analysis of the pull-off strength measurements, considering three selected factors frequently found in practice: the coring depth into substrate, the floor thickness and the concrete substrate class. These authors concluded that such factors affect the measurements results significantly.

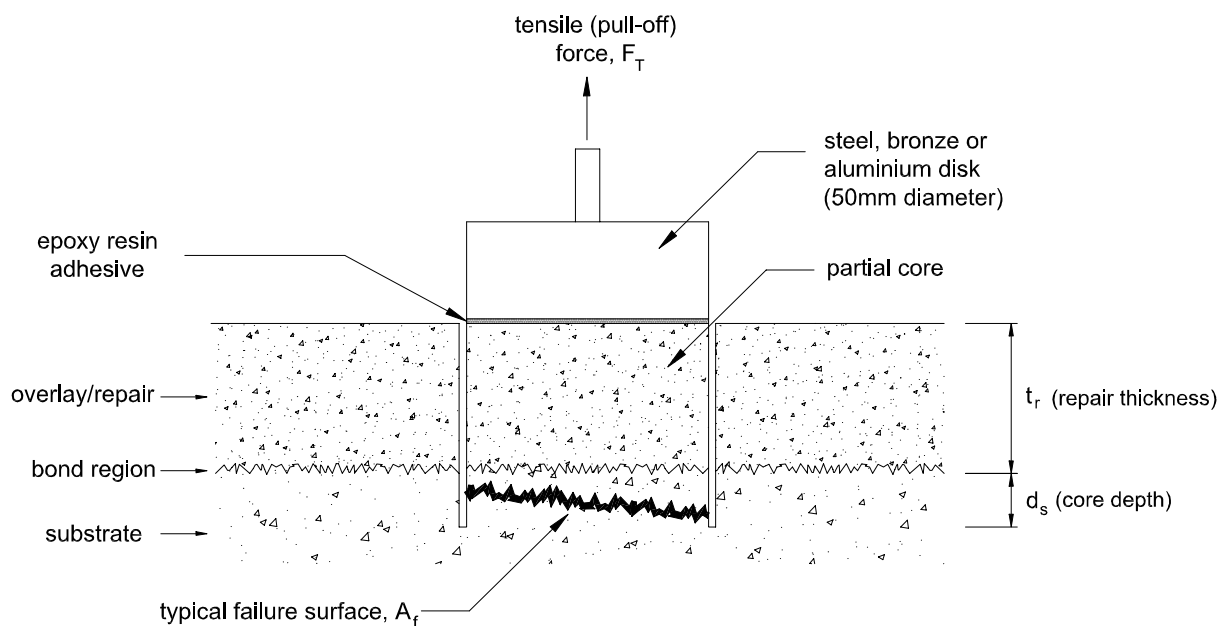


Figure 04 - Schematic representation of pull-off test principle.

To evaluate the adhesion strength of an adhesive material that bonds a concrete substrate to a concrete overlay, pull-off test is being widely used with a partial coring technique. As mentioned before, the pull-off test involves the application of a direct tensile load (F_T) to a partial core that mobilizes the repair material, the bond line and a portion of the substrate until failure occurs. The tensile load is applied to the partial core through the use of a metal, bronze or aluminium disk with a pull pin, bonded to the overlay with an epoxy resin. A loading device with a reaction frame applies the load to the pull pin at a constant rate. **Figure 04** illustrates the principle of the pull-off test.

The pull-off strength (S_{PO}) is defined as the tensile (pull-off) force (F_T) divided by the area of the fracture surface (A_f):

$$S_{PO} = \frac{F_T}{A_f}$$

There are several different types of in situ direct tensile tests proposed in the last years to evaluate the bond properties and the performance of repair materials in general. VAYSBURD and McDONALD (1999) provided a brief review of the most common tensile bond tests, as well as, an evaluation of three types of in situ direct tensile testing

equipment. They recommend the pull-off test, with partial coring, as the best available method for monitoring bond strengths in the field. One of the devices evaluated in their study includes the test equipment chosen for the present work, namely the Proceq DYNA Z15, with a 48 mm diameter disc (**Figure 05**). This equipment has a load capacity of 16kN, an accuracy < 2% and a resolution of 0.10 N/mm² (PROCEQ, 1998).



Figure 05 - Testing with Proceq DYNA Z15.

Even though there are variations in the testing equipment and in the method of carrying out the pull-off tests, the general procedures can be described as follows (ASTM D4541, 1995 and JSCE-E545, 2000):

- *definition and preparation of the test area.* The testing surface should be planed. The position of each test site should be determined taking into consideration the distance from the edges of the concrete slab specimen and the distance between the different test areas;
- *partial coring into the existing substrate, in the perpendicular direction to the repair surface;*
- *glue the disc to the core using an epoxy resin.* To attach the disc considerable care is needed in the surface preparation of the concrete. A suitable process to ensure good bonding of the adhesive should be adopted. For this purpose a curing period of time of about 24 hours is needed, but other periods of time might be used, depending on the material properties and environmental conditions (BUNGEY and MILLARD, 1986);
- *attach a loading frame to the disc.* The frame around the disc provides the reaction system to the applied load;

- *pull-off the disc* with a manual or hydraulic device following a specified loading rate, and measuring the force corresponding to the moment when the specimen failed.

After performing the test, the failure mode should be carefully analysed as it provides information about what was really measured. If a cohesive failure in the concrete substrate is detected, the entity evaluated is the tensile strength of the concrete substrate. If a cohesive failure in the overlay material is observed, the stress determined corresponds to the tensile strength of the repair overlay. Finally, if an adhesive failure between two materials is detected, it is the adhesion strength between the overlay and the substrate that is evaluated (CHMIELEWSKA et al, 2003).

The ASTM D4541 standard recommends that each test area must be separated by, at least, the distance needed to accommodate the detaching apparatus. However, the British Standard BS 1881: Part 207 advises that this distance should be, at least, two core-hole diameters and one diameter from the edge.

According to VAYSBURD and McDONALD (1999), an important issue associated with pull-off tests is the depth of the core drilling into the existing concrete substrate, and for the mentioned authors, ignoring the effect of the drilled depth may be one of the main causes of the difficulties in reproducing and comparing test results.

The partial core is usually cut by means of a rotary core cutting drill with diamond bits. To avoid cutting damage, and according to BUNGEY and MILLARD (1986), it is important to ensure uniform pressure when the core is being drilled through the concrete overlay into the substrate. This operation is mostly dependent on workmanship, thus it is essential that a skilled operator carry out the works.

Reducing the core diameter leads to an increasing influence of internal defects (in the concrete volume) in the specimen pull-off strength. Additionally, when reducing the core diameter, the ratio of cut surface area to volume increases and, at the same time, the intensity of damages occurring in the partial core drilling process increases (BUNGEY and MILLARD, 1986). Thus, it is expected that pull-off concrete strength decreases when reducing core diameter.

In general, the 50 mm core diameter is the most common in the specifications, being the maximum aggregate size not taken into account by the standards in the definition of the core diameter. A minimum ratio between the core diameter and the large aggregate ratio of three is generally recognized as acceptable for testing drilled concrete cores (BUNGEY and MILLARD, 1986).

In this work a core diameter of 48 mm with approximately 15 ± 5 mm of drilling depth into the substrate was adopted. These are common values adopted for, example, by AUSTIN et al. (1995). These authors analysed the effect of the depth on the pull-off strength and concluded that by decreasing the drilling depth, the stress concentrations increased, which results in a lower pull-off strength value. **Figure 06** illustrates the definition of the test area for the 15 mm deep substrate cores.

It is noted that there is also an agreement about the effects of the loading rate on the test results. Higher loading rates generally result in higher failure loads (AUSTIN et al., 1995), but no comprehensive work in this issue seems to be available in the literature. The loading rate adopted in this work follows the British Standard (BS 1881: Part 207, 1992 and BS EN 1542, 1999) suggestion of $0.05 \pm 0.01 \text{ MPa s}^{-1}$.

Finally, load eccentricity is another factor that affects the test results. According to AUSTIN et al., the load eccentricity in a partial core pull-off test depends basically on the orthogonality of the core drilling (relatively to the substrate) and accuracy in positioning the metal disc on top of the partial core. In this way, if the orthogonality of the core drilling is not guaranteed, the eccentricity of the loading will increase with the deepness of the core drilling. In the opinion of authors' of this work, it is expected that by increasing the drilling depth, the core damage generated by the vibration of the cutting drill machine increases.

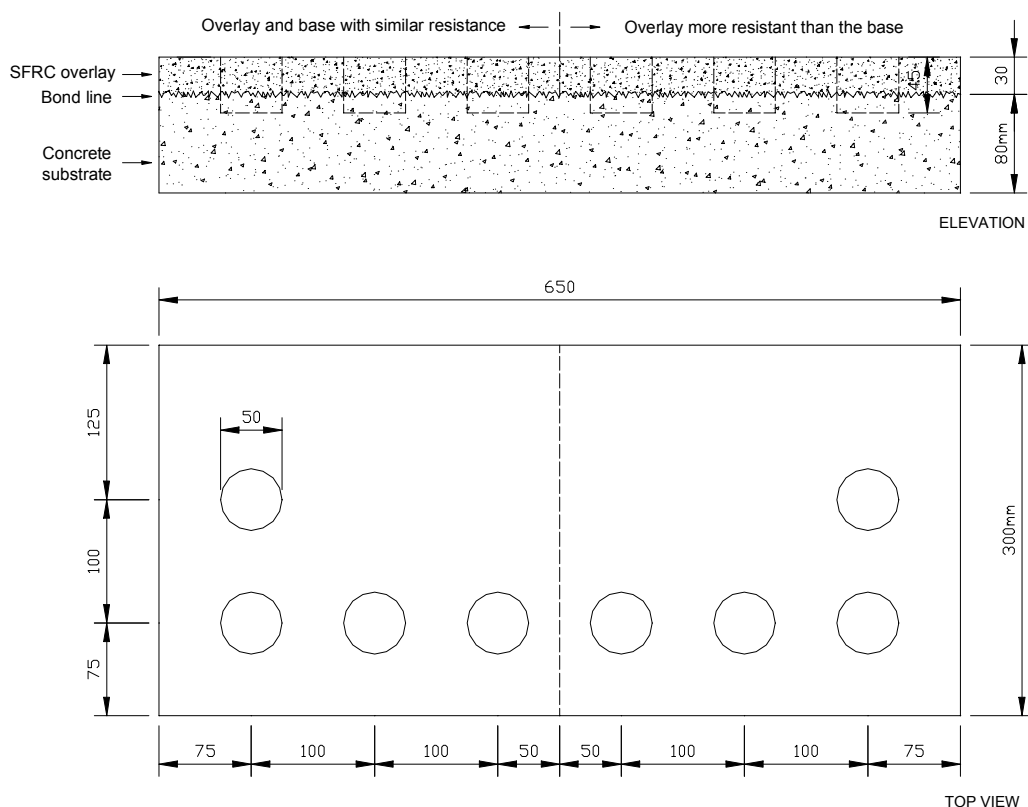


Figure 06 - Location of the cores used for pull-off tests (units in millimeters).

In this work, before gluing the disc using an epoxy resin, a very thin layer of the concrete surface was removed by a stone wear machine appropriate for this purpose (**Figure 07**). Afterwards, the concrete surface was cleaned and degreased, and the disc was cleaned with alcohol. Failure in the adhesive-concrete interface or disc-adhesive interface was never verified, confirming the excellent performance of the adopted procedure. Due to practical and economic reasons bronze discs have been selected for all tests.



(a)



(b)

Figure 07 - Removal of a very thin layer from the concrete surface, (a) overview of the machine and (b) detail of the stone wear device.

4 Results

The notation adopted to identify each specimen was the following: **BxCyPz**, where:

- B** = concrete base;
- x** = strength class designation of the concrete substrate (1, 2 and 3);
- C** = concrete overlay;
- y** = strength class designation of the concrete overlay (1, 2, 3, 4, 5 and 6). The **y'** is for the case of bond coat applied on saturated substrate surface;
- P** = bond product, and
- z** = type of bond product (1, 2 and 3).

Therefore, B2C4P3 refers to the specimen of concrete substrate of C40/50 grade, concrete overlay of class C50/60 bonded with the product type 3.

Tests Performed Manually with Proceq DYNA Z15

Tables 08, 09 and 10 show the pull-off test results for all the specimens, composed by the four pull-off strength results S_{PO} of each series, the average pull-off strength $S_{PO,m}$, the standard deviation (Std. dev.) and the coefficient of variation (COV).

The analysis of the COV of four test specimens for each bond material presented shows that it varies from 3.43 to 38.87 percent. The COV's for series B1C1'P3, B2C3P3, B2C4P3, B3C5P3, B3C4'P3 and B3C6P3 are relatively high and suggest that the test data are quite variable, while the COV's for the others models are acceptable, taking into consideration that this is a tensile test where significant scatter on the results is always affected.

The authors believe that the higher values of COV are not only due to the lack of precision of the test method, but also due to the intrinsic heterogeneity of granular materials like concrete. The difficulty on assuring always equal test procedures has also contributed for the large scatter.

Table 08 - Results of the pull-off tests in series of C20/30 strength class of the concrete base.

Model	Concrete age (days)		f _c (at 28 days in MPa)		Test	S _{PO} (MPa)	S _{PO,m} (MPa)	Std. dev. (MPa)	COV. (%)					
	Base	Layer	Base	Layer										
B1C1P1	64	29	22.32	25.87	1	1.55	1.48	0.14	9.46					
					2	1.41								
					3	1.33								
					4	1.63								
B1C1P2	66	31			25.87	1				1.48	1.58	0.18	11.39	
						2				1.83				
						3				1.57				
						4				1.43				
B1C1P3	68	33		25.87	25.87	1	1.19	1.12	0.09	8.04				
						2	0.99							
						3	1.18							
						4	1.11							
B1C1'P3	177	100	27.36 (55)	27.36 (55)	1	1.73	1.35	0.20	22.25					
					2	1.38								
					3	1.01								
					4	1.27								
B1C2P1	65	30	22.32	32.08	1	1.66	1.61	0.20	12.42					
					2	1.44								
					3	1.87								
					4	1.46								
B1C2P2	67	32			32.08	32.08				1	1.49	1.83	0.28	15.30
										2	1.84			
										3	2.17			
										4	1.83			
B1C2P3	69	34		32.08	32.08	1	1.56	1.36	0.16	11.76				
						2	1.16							
						3	1.37							
						4	1.37							
B1C2'P3	177	96	38.48 (52)	38.48 (52)	1	1.71	1.43	0.25	17.46					
					2	1.45								
					3	1.11								
					4	1.44								

Note: Coefficient of Variation (COV) = (Standard deviation/Average) x 100
(value) age at testing, when the test was not carried out at 28 days

Table 09 - Results of the pull-off tests in series of C40/50 strength class of the concrete base.

Model	Concrete age (days)		f _c (at 28 days in MPa)		Test	S _{PO} (MPa)	S _{PO,m} (MPa)	Std.dev. (MPa)	COV. (%)	
	Base	Layer	Base	Layer						
B2C3P1	69	30	42.59	41.50	1	1.99	2.46	0.37	15.04	
						2				2.33
						3				2.76
						4				2.74
B2C3P2	71	32				1	2.50	2.59	0.17	6.56
						2	2.75			
						3	2.39			
						4	2.71			
B2C3P3	74	35			1	1.71	1.69	0.41	24.26	
					2	1.35				
					3	2.27				
					4	1.44				
B2C2'P3	181	99		38.48 (52)	1	2.32	2.22	0.36	16.10	
				2	2.21					
				3	2.60					
				4	1.74					
B2C4P1	70	31	42.59	53.51	1	2.29	2.38	0.43	18.07	
						2				2.82
						3				1.82
						4				2.57
B2C4P2	73	34				1	2.50	2.35	0.28	11.91
						2	2.64			
						3	2.02			
						4	2.24			
B2C4P3	75	36			1	1.88	1.61	0.40	24.84	
					2	2.02				
					3	1.37				
					4	1.18				
B2C3'P3	181	96		58.46 (49)	1	1.52	1.81	0.24	13.22	
				2	1.85					
				3	2.10					
				4	1.77					

Note: Coefficient of Variation (COV) = (Standard deviation/Average) x 100
(value) age at testing, when the test was not carried out at 28 days

The average pull-off strength values are depicted in **Figure 08**, for all series. It can be seen that increasing the strength of the overlay does not lead to an increase of the pull-off strength. On the contrary, the strength of the substrate plays a major role in the pull-off strength. From the experimental data it is also possible to observe that the pull-off strength for bond product P3 is relatively low in comparison with the results for P1 and P2, meaning that the bond product plays a role in the response. The P2 bond material attained greater average pull-off strengths than the others bond materials, independently of the substrate and overlay compressive strength (**Figures 09** and **10**). **Figure 11** indicates linear increasing trend of pull-off strength with the compressive strength of concrete substrate and SFRC overlay.

Table 10 - Results of the pull-off tests in series of C60/70 strength class of the concrete base.

Bond characterization between concrete base and repairing SFRC by pull-off tests - 20/57

Model	Concrete age (days)		f _c (at 28 days in MPa)		Test	S _{PO} (MPa)	S _{PO,m} (MPa)	Std. dev. (MPa)	COV (%)	
	Base	Layer	Base	Layer						
B3C5P1	70	33	60.82	62.54	1	3.15	3.21	0.11	3.43	
						2				3.11
						3				3.21
						4				3.36
B3C5P2	72	35				1	4.59	4.20	0.27	6.43
						2	3.95			
						3	4.11			
						4	4.16			
B3C5P3	72	35			1	3.76	2.83	0.65	22.97	
					2	2.33				
					3	2.76				
					4	2.46				
B3C4'P3	175	96		64.34 (49)	1	3.15	2.57	0.53	20.51	
				2	2.87					
				3	2.21					
				4	2.04					
B3C6P1	70	33	60.82	64.38	1	3.55	3.32	0.52	15.66	
						2				2.78
						3				3.00
						4				3.93
B3C6P2	72	35				1	3.88	3.73	0.29	7.77
						2	3.72			
						3	3.33			
						4	3.98			
B3C6P3	75	38			1	2.17	2.47	0.96	38.87	
					2	1.33				
					3	2.78				
					4	3.61				
B3C5'P3	175	91		63.10 (44)	1	2.21	2.36	0.37	15.51	
				2	2.04					
				3	2.29					
				4	2.88					

Note: Coefficient of Variation (COV) = (Standard deviation/Average) x 100
(value) age at testing, when the test was not carried out at 28 days

A marginal benefit is verified when the bond coat product P3 is applied on saturated substrate surface for the cases of low and medium concrete class strength of the base (models B1C1', B1C2', B2C3' and B2C4'). For the case of high concrete class strength of the base (models B3C5' and B3C6'), a reduction in the pull-off strength was observed (**Figures 09 and 10**). The substrate of these series was made by the highest concrete strength class. This type of concrete has offered higher resistance to the penetration of the water used to saturate the substrate surface, resulting in the formation of a water film that has decreased the bond strength between the two concrete materials.

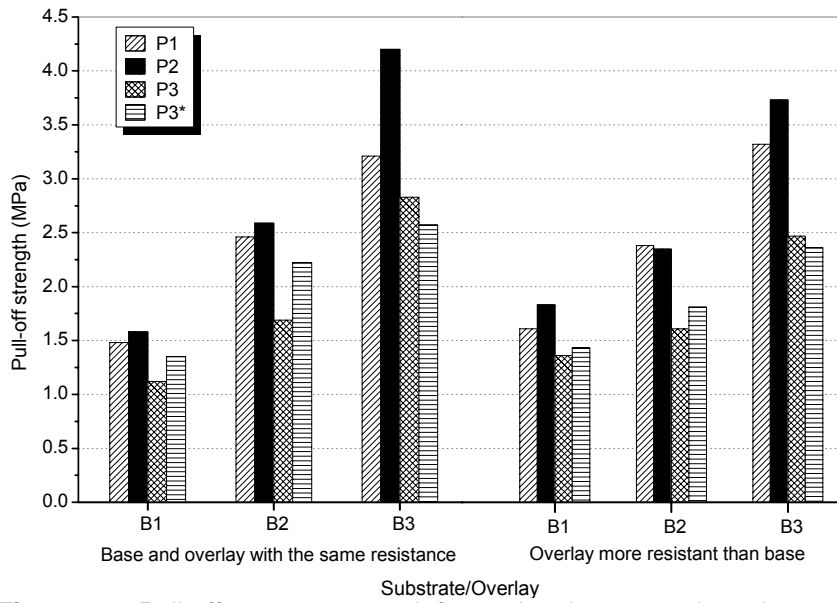


Figure 08 - Pull-off average strength for each substrate and overlay type. (where P3* indicates bond P3 applied on saturate substrate surface)

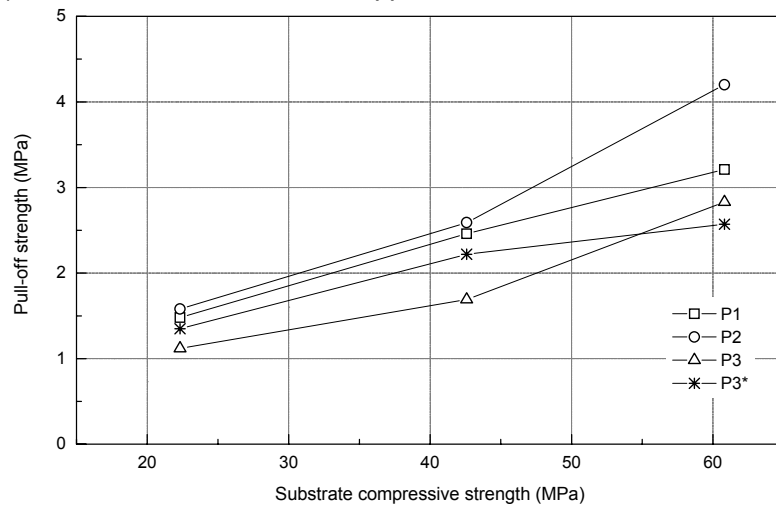


Figure 09 - Concrete overlay and concrete substrate with similar compressive strength. (where P3* indicates bond P3 applied on saturate substrate surface)

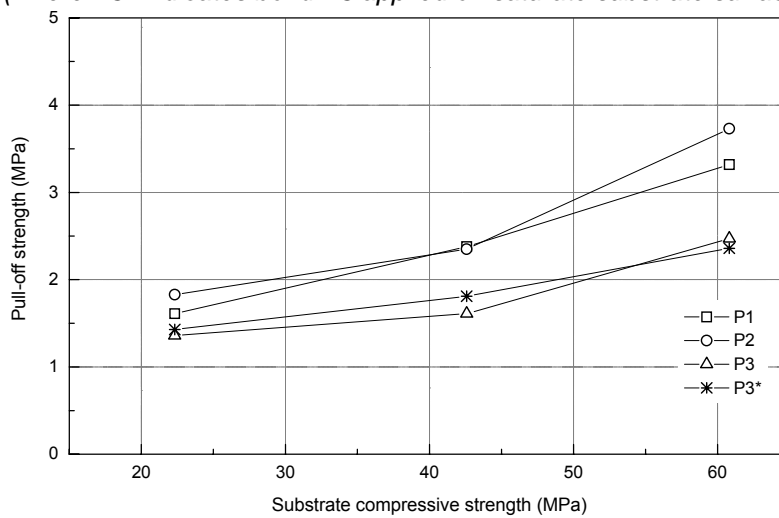


Figure 10 - Concrete overlay more resistant than the concrete base. (where P3* indicates bond P3 applied on saturated substrate surface)

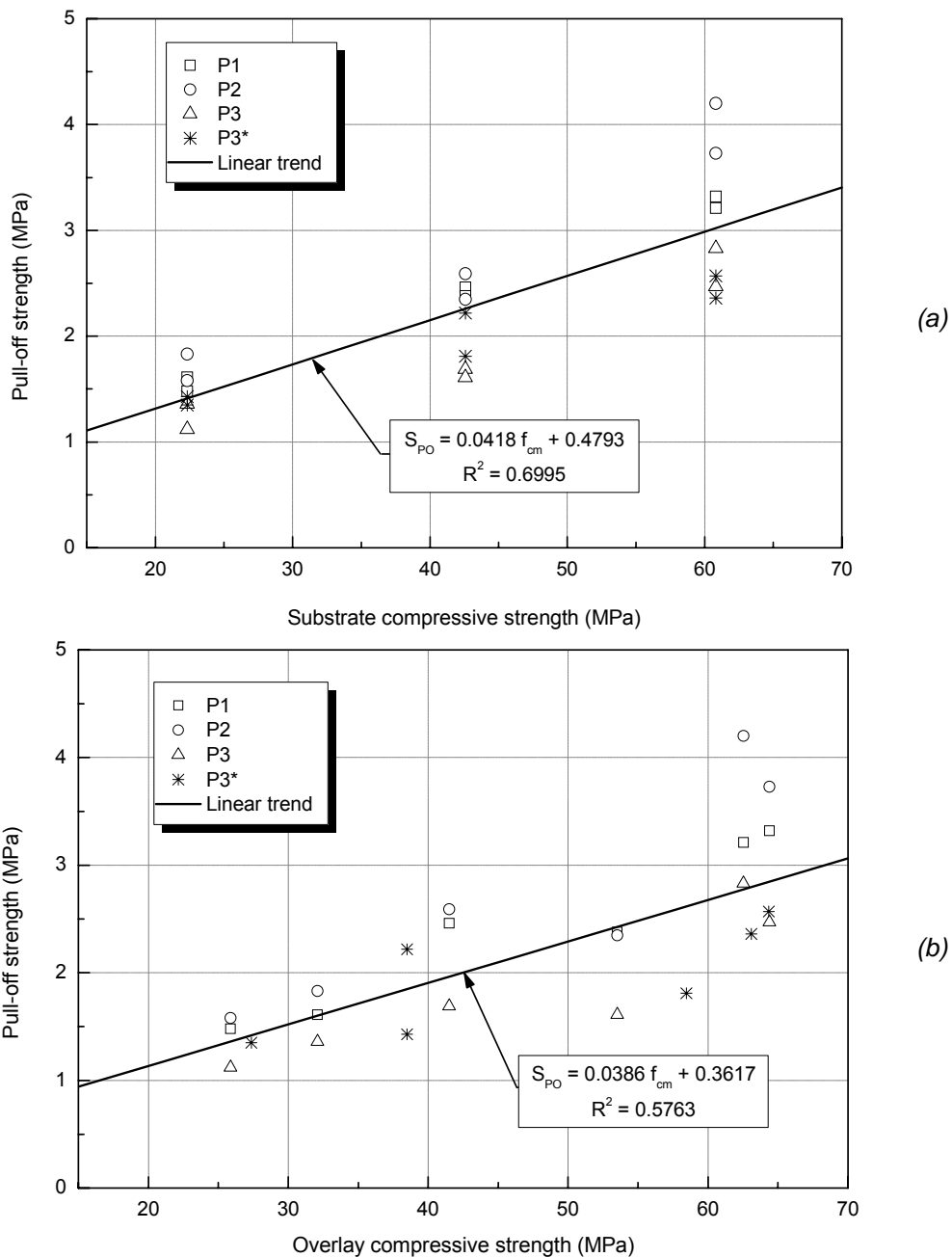


Figure 11 - Effect of substrate strength (a), and overlay strength (b), on the pull-off strength. (where P3* indicates bond P3 applied on saturated substrate surface)

The average pull-off strength for each model and also a performance / cost comparison are presented in **Table 11**. The analyses based on average pull-off strength demonstrate that for the six models the average pull-off strength obtained with bond material P2 is 1.11 and 1.46 (1.36) times higher than the average pull-off strength obtained with P1 and P3 (and P3 with saturated substrate surface) bond materials, respectively.

From the analysis of **Table 11** it is verified that, increasing the substrate strength the ratio of strength to cost is increased for the three bond agents, meaning that the substrate plays a key role in the response. For the stronger substrate, the performance is twice the value registered in the weak substrate.

The following expression was used for the computation of strength to cost ratio:

$$R_{SCi} = \frac{S_{POi}}{C_i \cdot A_{PO} \cdot d_i}$$

where:

- i is the bond coat product ($i=1, 2, 3$);
- R_{SCi} is the strength to cost ratio (MPa/€);
- S_{POi} = average pull-off strength (MPa);
- A_{PO} = area of the core with diameter of 48 mm (mm²);
- d_i = bond coat dosage (kg/mm²), and
- C_i = bond coat cost (€/kg).

Table 11 - Average pull-off strength, strength ratio and strength to cost ratio.

Model	Average pull-off strength (MPa)			Strength ratio		Strength to cost ratio ^(*)		
	Bond product			P2/P1	P2/P3	R _{SC1}	R _{SC2}	R _{SC3}
	P1	P2	P3					
B1C1	1.48	1.58	1.12 1.35 ⁽¹⁾	1.07	1.41 1.17 ⁽¹⁾	119	674	38 46
B1C2	1.61	1.83	1.36 1.43 ⁽²⁾	1.14	1.35 1.28 ⁽²⁾	130	780	47 49
B2C3	2.46	2.59	1.69 2.22 ⁽³⁾	1.05	1.53 1.17 ⁽³⁾	198	1104	58 76
B2C4	2.38	2.35	1.61 1.81 ⁽⁴⁾	0.99	1.46 1.30 ⁽⁴⁾	191	1002	55 62
B3C5	3.21	4.20	2.83 2.57 ⁽⁵⁾	1.31	1.48 1.63 ⁽⁵⁾	258	1791	97 88
B3C6	3.32	3.73	2.47 2.36 ⁽⁶⁾	1.12	1.51 1.58 ⁽⁶⁾	267	1590	85 81
Average				1.11	1.46 1.36			

⁽¹⁾ B1C1', ⁽²⁾ B1C2', ⁽³⁾ B2C2', ⁽⁴⁾ B2C3', ⁽⁵⁾ B3C4', ⁽⁶⁾ B3C5'

(*) taking into account the bond coat dosage (**Annex D**) and the area of the core. The prices were provided by the manufacturer (P1: 3.04€/Kg; P2: 1.44€/Kg; P3: 5.09€/Kg)

The better strength to cost ratio was obtained for the bond coat material P2, independently of the substrate and overlay compressive strength (**Figures 12 and 13**).

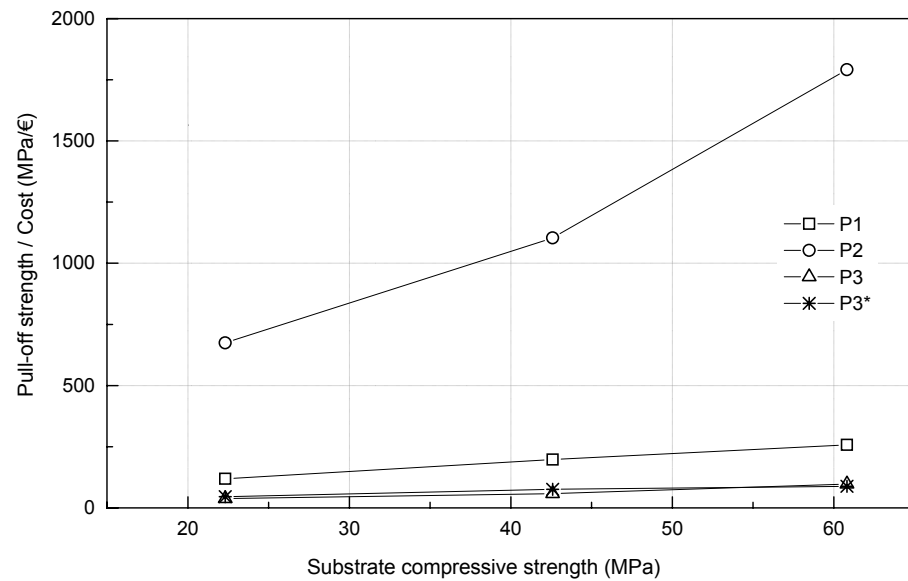


Figure 12 - Comparison of performance to cost ratio for concrete overlay and concrete substrate with similar compressive strength (where P3* indicates bond P3 applied on saturated substrate surface).

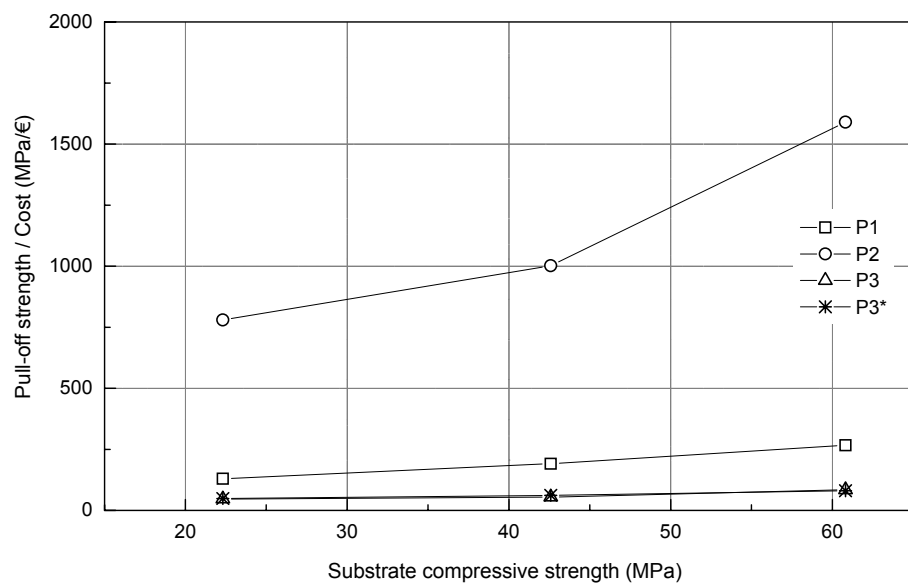


Figure 13 - Comparison of performance to cost ratio for concrete overlay more resistant than the concrete base (where P3* indicates bond P3 applied on saturated substrate surface).

As an example of the complex response of the pull-off test, **Figure 14** shows the fracture surface of core 2 of the model B1C1P2 (see **Table E2** of **Annex E**). The crack surface was initiated in the interface adhesive-concrete overlay from the zone where high percentage of voids and network voids were visible. This exceptional high percentage of voids might be related to the agglomeration and non-favourable fibre orientation. In spite of this apparent weakness, the pull-off strength of this specimen was the highest one of the specimens of its series. This extraneous result might be justified by the crack surface profile. In fact, after have been initiated at the adhesive-concrete overlay, the crack surface has crossed the adhesive layer, that has much higher tensile strength than the surrounded concrete materials, and ended at the concrete substrate, resulting a tortuous crack surface profile of higher surface.

Table 12 - Summary of the modes of failure.

Model	Bond product	Failure mode recorded
B1C1	1	Combination of substrate failure, aggregate-paste bond failure and paste failure.
	2	Existence of voids on the fracture surface.
	3	Failure in the bond-substrate interface.
	3 ⁽¹⁾	Substrate failure just below the bond-substrate interface (combination of paste failure, aggregate failure and aggregate-paste bond failure), and bond-overlay interface failure (in the high spots part of the substrate surface, i.e. in the stand out part of the coarse aggregates).
B1C2	1	Combination of substrate failure, aggregate-paste bond failure and paste failure. Existence of voids on the fracture surface.
	2	Combination of substrate failure, aggregate-paste bond failure, coarse aggregate failure and paste failure. Existence of voids on the fracture surface..
	3	Failure in the bond-substrate interface.
	3 ⁽²⁾	Substrate failure just below the bond-substrate interface (combination of paste failure, aggregate failure and aggregate-paste bond failure), and bond-overlay interface failure (in the high spots part of the substrate surface, i.e. in the stand out part of the coarse aggregates). Existence of voids on the fracture surface.
B2C3	1	Combination of substrate failure, aggregate-paste bond failure and paste failure. Existence of voids on the fracture surface.
	2	Failure in the substrate concrete just below the bond-substrate interface (top surface of substrate), aggregate-paste bond failure, coarse aggregate failure and paste failure. Existence of voids on the fracture surface.
	3	Failure in the bond-substrate interface.
	3 ⁽³⁾	Substrate failure just below the bond-substrate interface (combination of paste failure and aggregate failure), and bond-overlay interface failure (in the high spots part of the substrate surface, i.e. in the stand out part of the coarse aggregates).
B2C4	1	Combination of substrate failure, aggregate-paste bond failure and paste failure. Existence of voids on the fracture surface.
	2	Failure in the substrate concrete just below the bond-substrate interface (top surface of substrate), aggregate-paste bond failure, coarse aggregate failure and paste failure. Existence of voids on the fracture surface.
	3	Failure in the bond-substrate interface.
	3 ⁽⁴⁾	Failure in the bond-overlay interface (located in the high spots part of the substrate surface, i.e. in the stand out part of the coarse aggregates. A uniform bond-line thickness was not kept. Probably the remain water coat of the water used to saturated the surface changed the bond coat thixotropy and the adhesive drained away from the high spots and into the low spots) and failure in the bond-substrate interface (levelling to the top substrate surface in the paste and also in the coarse aggregates).
B3C5	1	Failure in the substrate concrete just below the bond-substrate interface (top surface of substrate), coarse aggregate failure and paste failure. Presence of voids on the fracture surface.
	2	Combination of substrate failure, bond-substrate failure, overlay failure and overlay-bond interface failure. Existence of voids on the fracture surface.
	3	Failure in the overlay-bond interface. Existence of voids on the fracture surface.
	3 ⁽⁵⁾	Bond-substrate interface failure and bond-overlay interface failure (in the high spots part of the substrate surface, i.e. in the stand out part of the coarse aggregates).
B3C6	1	Combination of substrate failure, just below the bond-substrate interface (top surface of substrate), aggregate-paste bond failure, coarse aggregate failure and paste failure. Existence of voids on the fracture surface.
	2	Combination of substrate failure, overlay-bond interface failure (presence of fibres in this region). Existence of voids on the fracture surface.
	3	Combination of bond-substrate interface failure, overlay-bond interface failure. Existence of voids on the fracture surface.
	3 ⁽⁶⁾	Bond-substrate interface failure and bond-overlay interface failure (in the high spots part of the substrate surface, i.e. in the stand out part of the coarse aggregates).

⁽¹⁾ B1C1', ⁽²⁾ B1C2', ⁽³⁾ B2C2', ⁽⁴⁾ B2C3', ⁽⁵⁾ B3C4', ⁽⁶⁾ B3C5'

The failure modes are summarized in **Table 12**. For complete reference the reader is referred to **Annex E**.



Figure 14 - Detail of the failure mode verified in the test 2 of the model B1C1P2.

Assessing the Influence of Loading Rate

To evaluate the influence of the loading rate on the pull-off strength, pull-off tests were carried out using two stress rates (0.02 and 0.15 MPa/s). For this purpose, the bond product P2 was selected, since it was verified to be the most effective one. A hydraulic servo-controlled actuator with a load cell of 25 kN capacity (accuracy to 0.1%) was employed for these tests (see **Figure 15**).

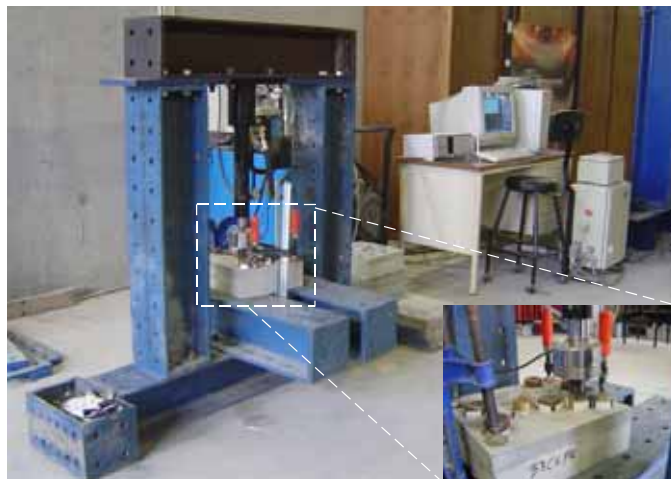


Figure 15 - Pull-off test setup for controlled loading rate.

For each of the six series of the experimental program, at least, 10 pull-off tests were carried out. The obtained results are resumed in **Figure 16**, where a tendency for the increase of the pull-off strength with the increase of the stress rate is shown. However, a confident conclusion can not be taken, since a large scatter was registered in the results. Several factors should have contributed for this scatter, namely: difficulty on assuming equal perfect pull-off test conditions; influence of differential shrinkage and cyclic action

of temperature variation (difficult to assure equal conditions, resulting distinct bond stresses in the interface between the two concrete layers); influence of the steel fibres distribution (impossible to guarantee equal conditions); influence of fly ash addition. The most uncharacteristic tendency was observed in series B3C6, where a pull-off strength decrease was obtained with the increase of the loading rate. In this series, the overlay is made by the highest concrete strength class, with 460 kg/m^3 of cement. This type of concrete is very sensitive to the influence of the curing conditions and temperature variations. Do not assuring equal conditions (which was the case since the specimens were submitted to the laboratory natural environmental conditions) distinct bond stress distributions occur in the interface between the two concrete layers, inducing different damage profiles. More details concerning the results can be found in **Annex F**.

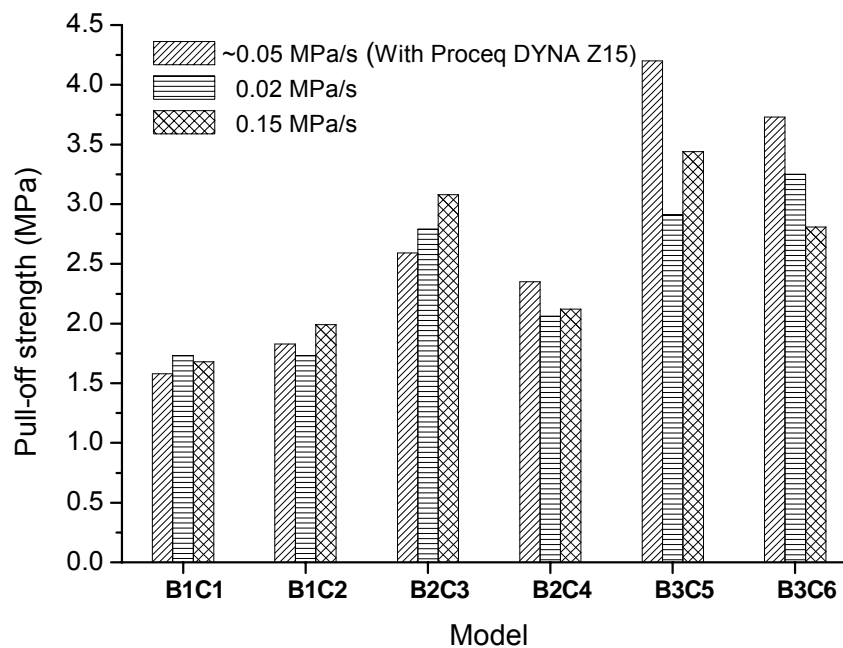


Figure 16 - Comparison of the pull-off strength for different stress rates.

5 Summary and Conclusions

An experimental campaign was conducted in order to: (a) investigate the effect of the concrete strength on bond strength between concrete substrate and concrete overlay, and (b) evaluate the bond performance of three commercially available bond agents, denoted as P1, P2 and P3. For this purpose a total of 285 partial-depth cores were tested.

The conclusions from this experimental study are the following:

- In general, all series have showed a large scatter in the pull-off tensile strength.
- Although this scatter, all bond coat materials exhibited an average pull-off strength higher than 1.12 MPa. For the concrete substrate of low and medium strength class, bonded by P1 or P2 adhesives, there was a clear tendency for failing by the concrete substrate failure, which indicates that, in these cases, the base concrete was generally the weakest link in the repair system. In this way, the pull-off strength reflects the tensile strength of the concrete substrate;
- For P1 and P2 bond materials the thin fibre reinforced concrete overlay was well bonded to the concrete substrate, and the tensile strength of the overlay has exceeded the tensile strength of the concrete substrate. Evidence of voids and non-uniform steel fibres distribution was observed in some failure surfaces (**Annex E**), suggesting that, additional attention should be given to the consolidating procedures of the fibre reinforced concrete mixture;
- The shape, maximum diameter and strength of coarse aggregates seem to have an important role in the pull-off strength, as for substrate of low / medium strength the crack surface was developed at the interface coarse aggregate-cement paste, while at substrates of high concrete strength the coarse aggregate was also crossed by the failure surface;
- In general, the failure surface was located at top of the substrate concrete, just below the bond adhesive. The lower resistance of the top surface of the substrate might explain this behaviour. The procedure adopted in the preparation of this zone might have been responsible for part of this weakness;
- The bond product P2 provided the highest pull-off strength values and, according to the manufacturer, was the more economical, being the best bond product for this type of application;



- The results accuse the existence of tendency for an increase of the pull-off strength with the increase of the test loading rate. The high dispersion registered in the obtained results, however, advises to be not conclusive, and recommends carrying out more experimental research with series of large number of specimens.



Acknowledgements

The authors acknowledge the financial support of the Portuguese Science and Technology Foundation (FCT), PhD grant number *SFRH / BD / 11232 / 2002*. Thanks also for the companies “Companhia Geral de Cal e Cimento S.A. (SECIL)”, Sika S.A., “Central do Pego”, “Pedreiras Bezerras”, Bekaert NV, “Bettor MBT Portugal Produtos Químicos para Construção S.A.”, that, generously, have supplied cement, bond products, fly ash, aggregates, steel fibres and superplasticizer, respectively.



References

- ACI 503R. Use of epoxy compounds with concrete, ACI Manual of Concrete Practice, Part 5, Reported by Committee 503, American Concrete Institute, 28 pp., 1993 (Reapproved 1998).
- ACI 503.2. Standard specification for bonding plastic concrete to hardened concrete with a multi-component epoxy adhesive, ACI Manual of Concrete Practice, Part 5, Reported by Committee 503, American Concrete Institute, 5 pp., 1992 (Reapproved 1997).
- ACI 503.5R. Guide for the selection of polymer adhesives with concrete, ACI Manual of Concrete Practice, Part 5, Reported by Committee 503, American Concrete Institute, 4 pp., 1997.
- ACI 503.6R. Guide for the application of epoxy and latex adhesives for bonding freshly mixed and hardened concretes, ACI Manual of Concrete Practice, Part 5, Reported by Committee 503, American Concrete Institute, 16 pp., 1992 (Reapproved 1997).
- ASTM D4541. Standard test method for pull-off strength of coating using portable adhesion testers, American Society for Testing and Materials, 1995.
- AUSTIN, S., ROBINS, P., and PAN, V. Tensile bond testing of concrete repairs, *Materials and Structures*, Vol. 28, pp. 249-259, 1995.
- BARROS, J. A. O., FIGUEIRAS, J. A. Experimental behaviour of fibre concrete slabs on soil. *Journal Mechanics of Cohesive-frictional Materials*, Vol. 3, pp. 277-290, 1998.
- BS 1881. Recommendations for the assessment of concrete strength by near-to-surface tests, Part 207, British Standard Institution, London, 1992.
- BS EN 1542. Products and systems for the protection and repair of concrete structures - Test methods - Measurement of bond strength by pull-off, British Standard Institution, London, 1999.
- BUNGEY, J. H.; MILLARD, S. G. Testing of concrete in structures, Chapman & Hall, Third Edition, Cambridge, Great Britain, April 1996.
- CEB-FIP MODEL CODE, Design code. Comité Euro-International du Béton, Bulletin d'Information CEB Lausanne, Switzerland, 1993.
- CHMIELEWSKA, B., CZARNECKI, L., and KRUPA, P. Influence of selected factors on the results of pull-off tests for industrial floors, 5th International Colloquium - Industrial Floors '03. Technische Akademie Esslingen, Jan. 21-23, 2003.



- COUTINHO, A. S. Manufacturing and properties of concrete, National Civil Engineering Laboratory, 3 volumes, Lisbon, Portugal, 1988. (in Portuguese)
- DELATTE, N. and SEHDEV, A. Mechanical properties and durability of BCO and UTW concrete, Annual Meeting of the TRB, 82th, Washington D.C., January, 2003. (Paper presented for the TRB annual meeting of 2003, Washington D.C.)
- DRAMIX: product data sheet, N. V. Bekaert S.A., 1998.
- FHA - Federal Highway Administration. Tensile bond strength of a high performance concrete bridge deck overlay, Field test report, Mobile Concrete Library Project # 9904, U.S. Department of Transportation home page, 2000.
<http://www.fhwa.dot.gov/pavement/mcl9904.pdf>. (available on March 21, 2003)
- JSCE-E 545. Test method for direct pull-off strength of continuous fibre sheets with concrete, Concrete Library of JSCE. Japan Society of Civil Engineers, Tokyo, Japan, 2000.
- KNAB, L. I. Factors related to the performance of concrete repair materials, Technical Report REMR-CS-12, US Army Corps of Engineers, Washington, DC, March, 1988.
- PROCEQ, Pull-off tester Dyna Z-16 datasheet. Proceq, S.A., Switzerland, 1998.
- SIKA, Technical data sheet - construction, Sika - Chemical Industry, S.A., Edition n° 5, 434 p., 2002. (in Portuguese)
- SPRINKEL, M. M., OZYILDIRIM, C. Evaluation of high performance concrete overlays placed on Route 60 over Lynnhaven Inlet in Virginia, Final Report, Virginia Transportation Research Council, Charlottesville, Virginia, 2000.
- VAYSBURD, A. M.; MACDONALD, J. E. An evaluation of equipment and procedures for tensile bond testing of concrete repairs, Technical Report REMR-CS-61, US Army Corps of Engineers, Washington, DC, Jun., 1999.



ANNEXES

Annex A - Physical properties of the aggregates

Annex B - Particle sizing of the aggregates

Annex C - Data of the compressive strength of the substrate concrete and of the SFRC overlay

Annex D - Bond coat dosage adopted and respective proportions

Annex E - Failure surface recorded

Annex F - Data of the tests for two controlled stress rates

Annex A - Physical properties of the aggregates

Table A1 - Specific gravity and water absorption of fine aggregate 4/11.

P_1	WEIGHT OF THE SAMPLE DRIED IN AIR	4795.2 g
P_2	WEIGHT OF THE SATURATED SAMPLE IN THE AIR WITH DRY SURFACE	4857.6 g
P_3	WEIGHT OF THE SATURATED SAMPLE IN WATER	3023.0 g
G_a	SPECIFIC GRAVITY OF THE WATER AT TEST TEMPERATURE	1000.0 kg/m ³
$\frac{P_1}{P_2 - P_3} \times G_a$	SPECIFIC GRAVITY OF THE DRY PARTICLES	2613.8 kg/m ³
$\frac{P_1}{P_1 - P_3} \times G_a$	SPECIFIC GRAVITY OF THE IMPERMEABLE MATERIAL OF PARTICLES	2705.8 kg/m ³
$\frac{P_2}{P_2 - P_3} \times G_a$	SPECIFIC GRAVITY OF SATURATED PARTICLES WITH DRY SURFACE	2647.8 kg/m ³
$\frac{P_2 - P_1}{P_1} \times 100$	ABSORPTION	1,3 %

Table A2 - Specific gravity and water absorption of coarse aggregate 11/16.

P_1	WEIGHT OF THE SAMPLE DRIED IN AIR	5324,0 g
P_2	WEIGHT OF THE SATURATED SAMPLE IN THE AIR WITH THE DRY SURFACE	5378,0 g
P_3	WEIGHT, IN WATER, OF THE SATURATED SAMPLE	3359,2 g
G_a	SPECIFIC GRAVITY OF THE WATER AT TEST TEMPERATURE	1000,0 kg/m ³
$\frac{P_1}{P_2 - P_3} \times G_a$	SPECIFIC GRAVITY OF THE DRY PARTICLES	2637.2 kg/m ³
$\frac{P_1}{P_1 - P_3} \times G_a$	SPECIFIC GRAVITY OF THE IMPERMEABLE MATERIAL OF PARTICLES	2709.7 kg/m ³
$\frac{P_2}{P_2 - P_3} \times G_a$	SPECIFIC GRAVITY OF SATURATED PARTICLES WITH DRY SURFACE	2664.0 kg/m ³
$\frac{P_2 - P_1}{P_1} \times 100$	ABSORPTION	1,0 %



Table A3 - Specific gravity and water absorption of fine river sand.

P_1	WEIGHT OF THE SATURATED SAMPLE WITH DRY SURFACE	500.1 g
P_2	WEIGHT OF THE FULL WATER BOTTLE	709.6 g
P_3	WEIGHT OF THE FULL BOTTLE WITH SATURATED SAMPLE AND WATER	1014.3 g
P_4	WEIGHT OF THE DRY SAMPLE	494.7 g
G_a	SPECIFIC GRAVITY OF THE WATER AT TEST TEMPERATURE	1000.0 kg/m ³
$\frac{P_4}{P_1 + P_2 - P_3} \times G_a$	SPECIFIC GRAVITY OF THE DRY PARTICLES	2532.6 kg/m ³
$\frac{P_4}{P_4 + P_2 - P_3} \times G_a$	SPECIFIC GRAVITY OF THE IMPERMEABLE MATERIAL OF PARTICLES	2604.3 kg/m ³
$\frac{P_1}{P_1 + P_2 - P_3} \times G_a$	SPECIFIC GRAVITY OF SATURATED PARTICLES WITH DRY SURFACE	2560.1 kg/m ³
$\frac{P_1 - P_4}{P_4} \times 100$	ABSORPTION	1,1 %

Table A4 - Specific gravity and water absorption of coarse river sand.

P_1	WEIGHT OF THE SATURATED SAMPLE WITH DRY SURFACE	500.0g
P_2	WEIGHT OF THE FULL WATER BOTTLE	709.6 g
P_3	WEIGHT OF THE FULL BOTTLE WITH THE SATURATED SAMPLE AND WATER	1006.6 g
P_4	WEIGHT OF THE DRY SAMPLE	491.3 g
G_a	SPECIFIC GRAVITY OF THE WATER AT TEST TEMPERATURE	1000.0 kg/m ³
$\frac{P_4}{P_1 + P_2 - P_3} \times G_a$	SPECIFIC GRAVITY OF DRY PARTICLES	2420.3 kg/m ³
$\frac{P_4}{P_4 + P_2 - P_3} \times G_a$	SPECIFIC GRAVITY OF THE IMPERMEABLE MATERIAL OF PARTICLES	2528.3 kg/m ³
$\frac{P_1}{P_1 + P_2 - P_3} \times G_a$	SPECIFIC GRAVITY OF SATURATED PARTICLES WITH DRY SURFACE	2463.1 kg/m ³
$\frac{P_1 - P_4}{P_4} \times 100$	ABSORPTION	1,8 %

Annex B - Particle sizing of the aggregates

Table B1 - Sieve analysis of the fine river sand.

Sieve		Weight retained	% Retained	% Accumulated Retained	% Pass
n ^o	(mm)				
1"	25.400				
3/4"	19.100				
1/2"	12.700				
3/8"	9.520				
4"	4.760				
8"	2.380				100
16"	1.190	16.46	1.55	1.55	98.45
30"	0.595	81.47	7.66	9.21	90.79
50"	0.297	516.96	48.60	57.80	42.20
100"	0.149	283.82	26.68	84.48	15.52
200"	0.074	109.50	10.29	94.77	5.23
RESIDUE		55.61	5.23	100	0
TOTAL		1063.81		100	

$D_{max} = 1.31$ mm, according to COUTINHO (1988)

Table B2 - Sieve analysis of the coarse river sand.

Sieve		Weight retained	% Retained	% Accumulated Retained	% Pass
n ^o	(mm)				
1"	25.400				
3/4"	19.100				
1/2"	12.700				
3/8"	9.520				100
4"	4.760	18.80	1.88	1.88	98.12
8"	2.380	130.70	13.06	14.94	85.06
16"	1.190	259.50	25.94	40.88	59.12
30"	0.595	279.70	27.96	68.84	31.16
50"	0.297	205.90	20.58	89.42	10.58
100"	0.149	100.20	10.01	99.43	0.57
200"	0.074	5.30	0.53	99.96	0.04
RESIDUE		0.40	0.04	100	0
TOTAL		1000.50		100	

$D_{max} = 5.10$ mm, according to COUTINHO (1988)

Table B3 - Sieve analysis of the fine aggregate 4/11.

Sieve		Weight retained	% Retained	% Accumulated Retained	% Pass
n ^o	(mm)				
1"	25.400				
3/4"	19.100				100
1/2"	12.700				
3/8"	9.520	64.30	2.14	2.14	97.86
4"	4.760	1977.00	65.92	68.07	31.93
8"	2.380	802.80	26.77	94.83	5.17
16"	1.190	61.40	2.05	96.88	3.12
30"	0.595	22.10	0.74	97.62	2.38
50"	0.297	15.50	0.52	98.14	1.86
100"	0.149	17.20	0.57	98.71	1.29
200"	0.074	30.40	1.01	99.72	0.28
RESIDUE		8.30	0.28	100	0
TOTAL		2999.00		100	

$D_{max} = 9.60$ mm, according to COUTINHO (1988)

Table B4 - Sieve analysis of the coarse aggregate 11/16.

Sieve		Weight retained	% Retained	% Accumulated Retained	% Pass
n ^o	(mm)				
1"	25.400				
3/4"	19.100				100
1/2"	12.700	495.16	14.16	14.16	85.84
3/8"	9.520	1855.12	53.05	67.21	32.79
4"	4.760	1080.73	30.91	98.12	1.88
8"	2.380	21.20	0.61	98.72	1.28
16"	1.190	3.60	0.10	98.83	1.17
30"	0.595	2.63	0.08	98.90	1.10
50"	0.297	4.11	0.12	99.02	0.98
100"	0.149	7.95	0.23	99.25	0.75
200"	0.074	11.18	0.32	99.57	0.43
RESIDUE		15.19	0.43	100	0
TOTAL		3496.87		100	

$D_{max} = 14.35$ mm, according to COUTINHO (1988)

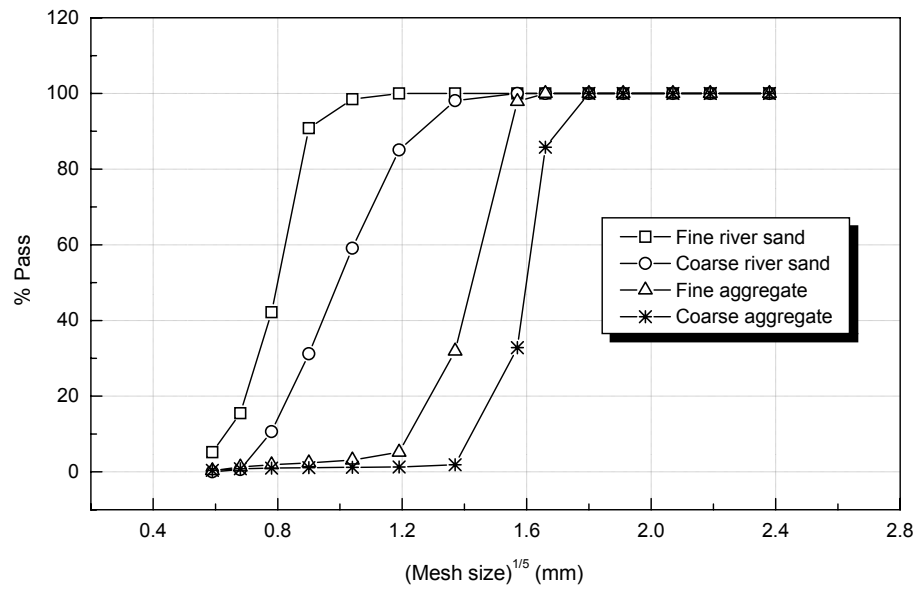


Figure B1 - Sieve analysis of the aggregates.

Annex C - Data of the compressive strength of the substrate concrete and of the SFRC overlay

Table C1 - Substrate concrete compressive strength at 28 days.

Designation	Test	f_c (MPa)	f_{cm} (MPa)	Std. dev. (MPa)	COV (%)
B1 (C16/20)	1	22.18	22.32	0.89	3.98
	2	23.27			
	3	21.51			
B2 (C35/45)	1	42.21	42.59	0.57	1.33
	2	43.24			
	3	42.31			
B3 (C55/67)	1	61.47	60.82	1.64	2.69
	2	58.96			
	3	62.04			

Note: Coefficient of Variation (COV) = (Standard deviation/Average) x 100.

Table C2 - Overlay concrete compressive strength at 28 days.

Designation	Test	f_c (MPa)	f_{cm} (MPa)	Std. dev. (MPa)	COV (%)
C1 (C20/25)	2	26.08	25.87	0.28	1.07
	2	25.56			
	3	25.98			
C2 (C25/30)	1	33.61	32.08	1.40	4.37
	2	31.79			
	3	30.85			
C3 (C35/45)	1	41.28	41.50	0.29	0.70
	2	41.39			
	3	41.83			
C4 (C45/55)	1	52.55	53.51	1.13	2.12
	2	53.21			
	3	54.76			
C5 (C55/67)	1	60.44	62.54	1.82	2.91
	2	63.53			
	3	63.66			
C6 (C60/75)	1	59.52	64.38	4.21	6.54
	2	66.91			
	3	66.70			

Note: Coefficient of Variation (COV) = (Standard deviation/Average) x 100.

Table C3 - Overlay concrete compressive strength.

Designation	Test	f_c (MPa)	f_{cm} (MPa)	Std. dev. (MPa)	COV (%)
C1' (C20/25)	1	27.10	27.36 (55)	0.55	2.02
	2	27.99			
	3	26.98			
C2' (C30/37)	1	40.25	38.48 (52)	2.11	5.47
	2	36.09			
	3	37.33			
	4	40.25			
C3' (C50/60)	1	58.01	58.46 (49)	0.92	1.57
	2	59.81			
	3	58.24			
	4	57.79			
C4' (C55/67)	1	64.98	64.34 (49)	4.82	7.49
	2	67.79			
	3	67.23			
	4	57.34			
C5' (C60/75)	1	62.06	63.10 (44)	4.76	7.54
	2	69.93			
	3	58.91			
	4	61.50			

Note: Coefficient of Variation (COV) = (Standard deviation/Average) x 100
(value) age at testing



Annex D - Bond coat dosage adopted and respective proportions

ICOSIT[®] K 101 (P1)

Dosage = 2.26 kg/m²

Component A = 193.6 g

Component B = 26.4 g

SIKADUR[®] 32 N (P2)

Dosage = 0.90 kg/m²

Component A = 58.66 g

Component B = 29.34 g

SIKATOP[®] ARMATEC 110 EPOCEM[®] (P3)

Dosage = 3.17 kg/m²

Component A = 18.06 g

Component B = 43.35 g

Component C = 247.50 g

Annex E - Failure surface recorded

Table E1- Modes and details of failure verified in B1C1P1 and B1C2P1 models.

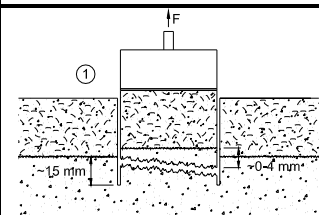
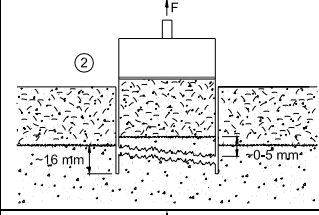
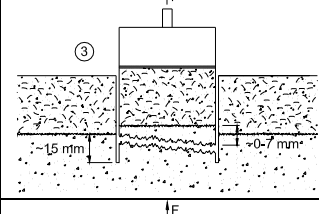
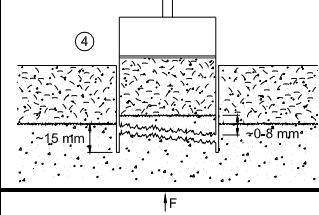
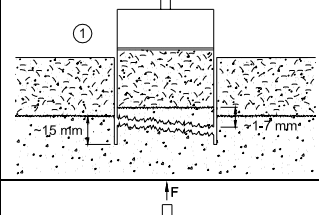
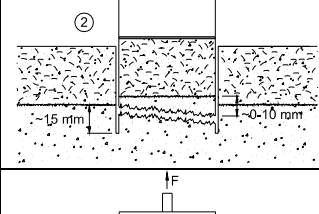
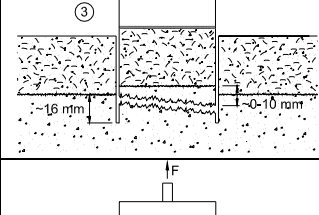
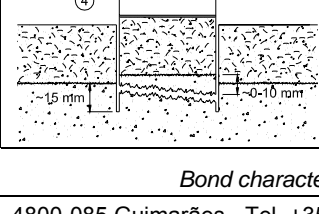
Model	Failure surface sketch	Details of the failure surface
B1C1P1		<p>Substrate failure: combination of paste failure and aggregate-paste bond failure in 6 coarse aggregates; Existence of 4 voids with $\phi \approx 2$ mm; Existence of 3 voids with $\phi \approx 1$ mm; Existence of other small voids.</p>
		<p>Substrate failure: combination of paste failure and aggregate-paste bond failure in 4 coarse aggregates; Existence of voids with $\phi < 1$ mm;</p>
		<p>Substrate failure: combination of paste failure and aggregate-paste bond failure in 6 coarse aggregates; Existence of 1 void with $\phi \approx 2.5$ mm; Existence of 6 voids with $\phi \approx 1$ mm; Existence of other small voids.</p>
		<p>Substrate failure: combination of paste failure and aggregate-paste bond failure in 8 coarse aggregates; Existence of 2 voids with $\phi \approx 2$ mm; Existence of other small voids.</p>
B1C2P1		<p>Substrate failure: combination of paste failure and aggregate-paste bond failure in 3 coarse aggregates; Existence of 2 voids with $\phi \approx 2.5$ mm; Existence of 6 voids $\phi \approx 1$ mm; Existence of other small voids.</p>
		<p>Substrate failure: combination of paste failure and aggregate-paste bond failure in 6 coarse aggregates; Existence of 3 voids with $\phi \approx 2.5$ mm; Existence of 8 voids with $\phi \approx 1$ mm; Existence of other small voids.</p>
		<p>Substrate failure: combination of paste failure and aggregate-paste bond failure in 6 coarse aggregates; Existence of 4 voids with $\phi \approx 1.5$ mm; Existence of other small voids.</p>
		<p>Substrate failure: combination of paste failure and aggregate-paste bond failure in 7 coarse aggregates; Existence of 4 voids with $\phi \approx 1.5$ mm; Existence of other small voids.</p>

Table E2 - Modes and details of failure verified in B1C1P2 and B1C2P2 models.

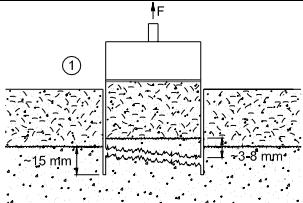
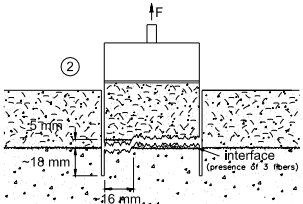
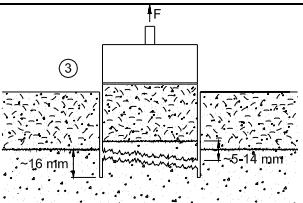
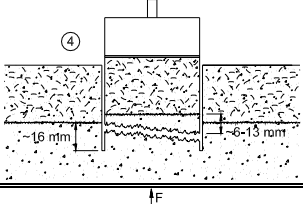
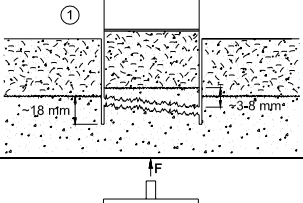
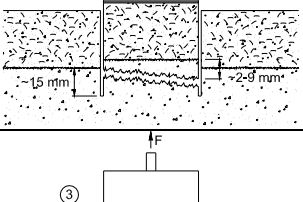
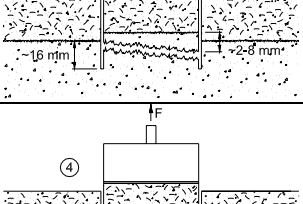
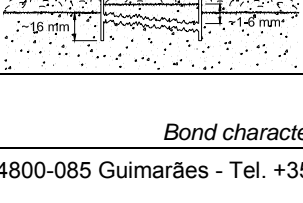
Model	Failure surface sketch	Details of the failure surface
B1C1P2		<p>Substrate failure: combination of paste failure and aggregate-paste bond failure in 3 coarse aggregates; Existence of 2 voids with $\phi \approx 2$ mm; Existence of 2 voids with $\phi \approx 1.5$ mm; Existence of 1 voids with $\phi \approx 7$ mm; Existence of other small voids.</p>
		<p>Substrate failure and just above the bond-overlay interface (with part of 3 fibres and significant amount of entrapped air voids, indicating that SFRC overlay was not properly consolidates); In the bond-overlay interface failure region: - Existence of 21 mm of 1 steel fibre; - Existence of 20 mm of 1 steel fibre; - Existence of 16 mm of 1 steel fibre; In the substrate failure region: - Existence of 1 void with $\phi \approx 8$ mm; - Existence of 1 void with $\phi \approx 2$ mm.</p>
		<p>Substrate failure: combination of paste failure and aggregate-paste bond failure in 4 coarse aggregates; Existence of 3 voids with $\phi \approx 2$ mm; Existence of other small voids.</p>
		<p>Substrate failure: combination of paste failure and aggregate-paste bond failure in 5 coarse aggregates; Existence of 7 voids with $\phi \approx 3$ mm; Existence of other small voids.</p>
B1C2P2		<p>Substrate failure: combination of paste failure and aggregate-paste bond failure in 8 coarse aggregates; Existence of 2 voids with $\phi \approx 5$ mm; Existence of 2 voids with $\phi \approx 2$ mm; Existence of other small voids.</p>
		<p>Substrate failure: combination of paste failure, coarse aggregate failure and aggregate-paste bond failure in 5 coarse aggregates; Existence of 2 voids with $\phi \approx 2$ mm; Existence of other small voids.</p>
		<p>Substrate failure: combination of paste failure, coarse aggregate failure and aggregate-paste bond failure in 3 coarse aggregates; Existence of 3 voids with $\phi \approx 1.5$ mm.</p>
		<p>Substrate failure: combination of paste failure and aggregate-paste bond failure in 4 coarse aggregates; Existence of 4 voids with $\phi \approx 1.5$ mm; Existence of other small voids.</p>

Table E3 - Modes and details of failure verified in B1C1P3 and B1C2P3 models.

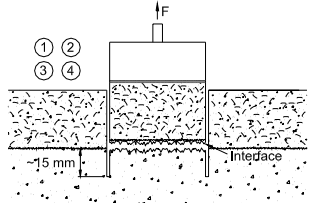
Model	Failure surface sketch	Details of the failure surface
B1C1P3 and B1C2P3		Failure in the bond-substrate interface.

Table E4 - Modes and details of failure verified in B2C3P1 and B3C4P1 models.

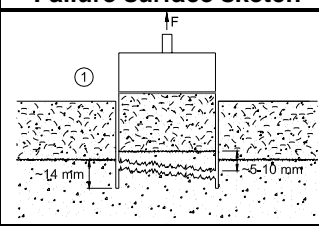
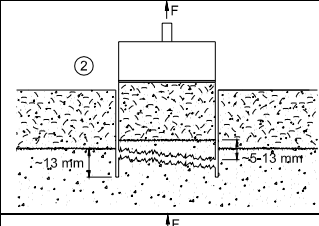
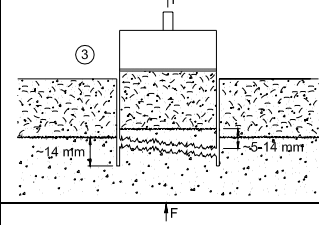
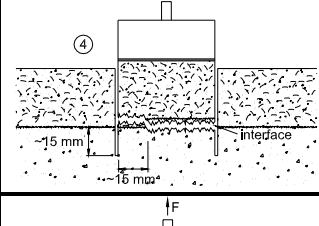
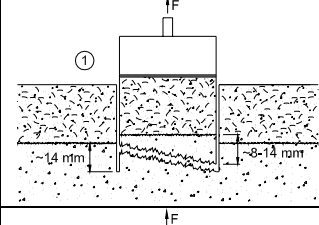
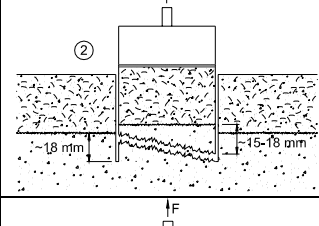
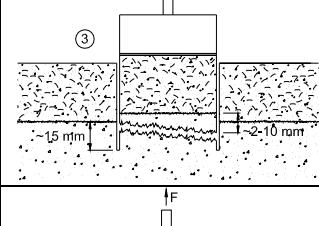
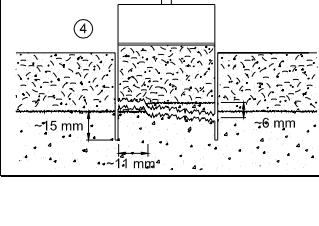
Model	Failure surface sketch	Details of the failure surface
B2C3P1		<p>Substrate failure: combination of paste failure, coarse aggregate failure and aggregate-paste bond failure in 5 coarse aggregates; Existence of 2 voids with $\phi \approx 4$ mm; Existence of 3 voids with $\phi \approx 2.5$ mm; Existence of others small voids with $\phi \approx 1$ mm.</p>
		<p>Substrate failure: combination of paste failure and coarse aggregate-paste bond failure; Existence of 3 voids with $\phi \approx 2$ mm; Existence of other voids with $\phi \leq 1.5$ mm; Existence of other small voids.</p>
		<p>Substrate failure: combination of paste failure and aggregate-paste bond failure in 4 coarse aggregates; Existence of 4 voids with $\phi \approx 1.5$ mm; Existence of other voids with $\phi \approx 1$ mm; Existence of other small voids.</p>
		<p>Substrate failure (combination of paste failure and aggregate-paste bond failure in 2 coarse aggregates), bond-substrate interface failure and bond-overlay interface failure; Existence of 5 voids with $\phi \approx 2$ mm; Existence of other small voids.</p>
B2C4P1		<p>Substrate failure: combination of paste failure and aggregate-paste bond failure in 4 coarse aggregates; Existence of 8 voids with $\phi \approx 4$ mm; Existence of other voids with $\phi_{\min} \approx 1$ mm and $\phi_{\max} \approx 3$ mm.</p>
		<p>Substrate failure: combination of paste failure and aggregate-paste bond failure in 3 coarse aggregates; Existence of 3 voids with $\phi \approx 6$ mm; Existence of 3 voids with $\phi \approx 3$ mm; Existence of other voids with $\phi_{\min} \approx 1$ mm and $\phi_{\max} \approx 2.5$ mm.</p>
		<p>Substrate failure: combination of paste failure and aggregate-paste bond failure in 3 coarse aggregates; Existence of 3 voids with $\phi \approx 2$ mm; Existence of 1 voids with $\phi \approx 5$ mm; Existence of other small voids.</p>
		<p>Substrate failure (aggregate-paste bond failure in 2 coarse aggregates) and just above the bond-overlay interface (existence of 10 mm of one steel fibre in this region); Existence of 5 voids with $\phi \approx 3$ mm; Existence of other small voids.</p>

Table E5 - Modes and details of failure verified in B2C3P2 and B3C4P2 models.

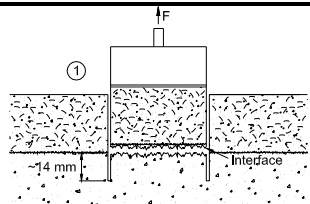
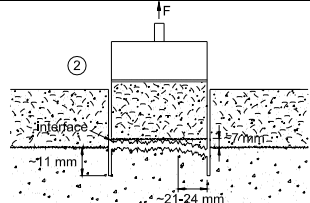
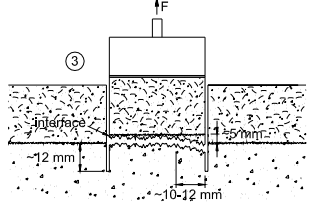
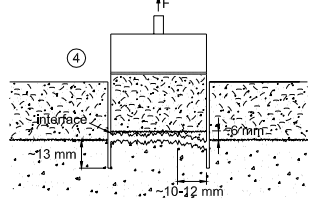
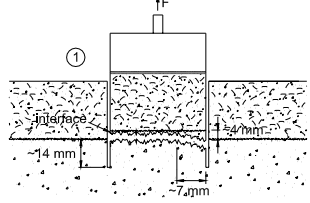
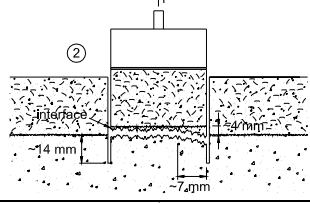
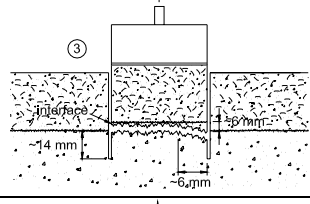
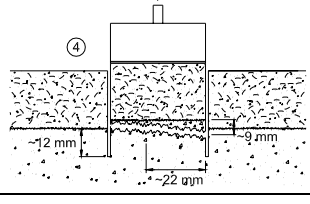
Model	Failure surface sketch	Details of the failure surface
B2C3P2		<p>Failure just below the bond-substrate interface (top surface of substrate): combination of paste failure, coarse aggregate failure and aggregate-paste bond failure; Existence of 2 voids with $\phi \approx 2$ mm; Existence of other small voids with $\phi \approx 1$ mm.</p>
		<p>Substrate failure and just below the bond-substrate interface: combination of paste failure, coarse aggregate failure and aggregate-paste bond failure; Existence of 4 voids with $\phi \approx 3.5$ mm; Existence of other voids with $\phi_{\min} \approx 1$ mm and $\phi_{\max} \approx 1.5$ mm.</p>
		<p>Substrate failure and just below the bond-substrate interface: combination of paste failure and coarse aggregate failure; Existence of 2 voids with $\phi \approx 1.5$ mm; Existence of other voids with $\phi \approx 1$ mm.</p>
		<p>Substrate failure and just below the bond-substrate interface: combination of paste failure and coarse aggregate failure; Existence of 1 voids with $\phi \approx 3.5$ mm; Existence of 1 voids with $\phi \approx 1$ mm; Existence of other small voids.</p>
B2C4P2		<p>Substrate failure (combination of paste failure, coarse aggregate failure and aggregate-paste bond failure) and just below the bond-substrate interface; Existence of 4 voids with $\phi \approx 1$ mm; Existence of other small voids.</p>
		<p>Substrate failure (combination of paste failure, coarse aggregate failure and aggregate-paste bond failure) and just below the bond-substrate interface; Existence of 1 voids with $\phi \approx 2$ mm; Existence of other small voids.</p>
		<p>Substrate failure (combination of paste failure, coarse aggregate failure and aggregate-paste bond failure) and just below the bond-substrate interface; Existence of 1 voids with $\phi \approx 1.5$ mm; Existence of other voids with $\phi \approx 1$ mm.</p>
		<p>Substrate failure (combination of paste failure and aggregate-paste bond failure) and just below the bond-substrate interface; Existence of 3 voids with $\phi \approx 3$ mm; Existence of 3 voids with $\phi \approx 1$ mm; Existence of other small voids.</p>

Table E6 - Modes and details of failure verified in B2C3P2 and B3C4P2 models.

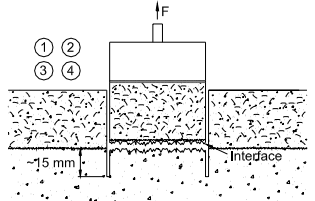
Model	Failure surface sketch	Details of the failure surface
B2C3P3 and B2C4P3		Failure in the bond-substrate interface.

Table E7 - Modes and details of failure verified in B3C5P1 and B3C6P1 models.

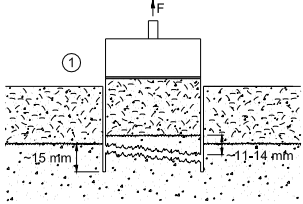
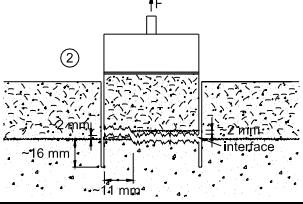
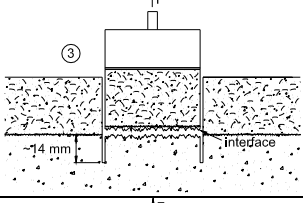
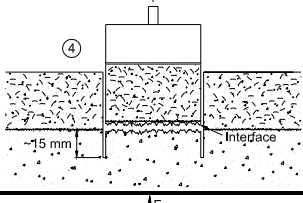
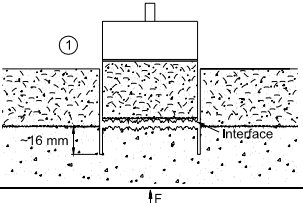
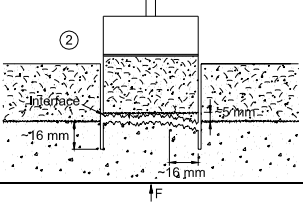
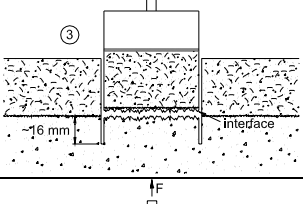
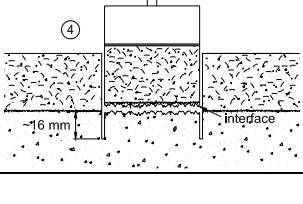
Model	Failure surface sketch	Details of the failure surface
B3C5P1		<p>Substrate failure: combination of paste failure and aggregate-paste bond failure in 6 coarse aggregates; Existence of 8 voids with $\phi \approx 2$ mm; One "leg" of the three equipment reaction frame moved during the test, probably introducing eccentricity.</p>
		<p>Substrate failure just below the bond-substrate interface (combination of paste failure and coarse aggregate failure), and overlay failure just above the bond-overlay interface; Existence of 2 voids with $\phi \approx 1.5$ mm; Existence of 1 void with $\phi \approx 5$ mm; Existence of 5 voids with $\phi \approx 1$ mm; Existence of other small voids.</p>
		<p>Substrate failure just below the bond-substrate interface (combination of paste failure and coarse aggregate failure); Existence of 1 void with $\phi \approx 2.5$ mm; Existence of other small voids.</p>
		<p>Substrate failure just below the bond-substrate interface (combination of paste failure and coarse aggregate failure); Existence of 3 voids with $\phi \approx 1.5$ mm; Existence of 1 void with $\phi \approx 3$ mm; Existence of other small voids.</p>
B3C6P1		<p>Substrate failure just below the bond-substrate interface (combination of paste failure and aggregate-paste bond failure in 1 coarse aggregate); Existence of voids with $\phi_{min} \approx 1$ mm and $\phi_{max} \approx 3$ mm; Existence of other small voids.</p>
		<p>Substrate failure and failure just below the bond-substrate interface (combination of paste failure, coarse aggregate failure and aggregate-paste bond failure); Existence of 1 void with $\phi \approx 3$ mm; Existence of 5 voids with $\phi \approx 1.5$ mm Existence of other small voids.</p>
		<p>Failure just below the bond-substrate interface (combination of paste failure and coarse aggregate failure); Existence of 7 voids with $\phi \approx 2$ mm; Existence of other small voids.</p>
		<p>Failure just below the bond-substrate interface (combination of paste failure and coarse aggregate failure); Existence of 2 voids with $\phi \approx 4$ mm; Existence of other small voids with $\phi_{min} \approx 1$ mm and $\phi_{max} \approx 2$ mm;</p>

Table E8 - Modes and details of failure verified in B3C5P2 and B3C6P2 models.

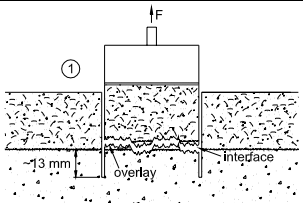
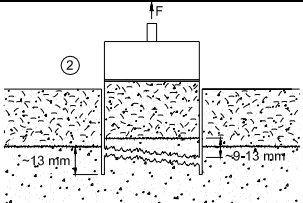
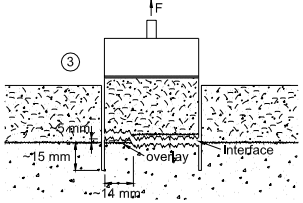
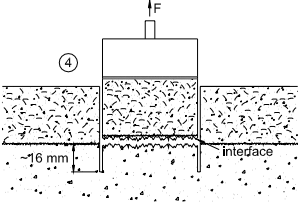
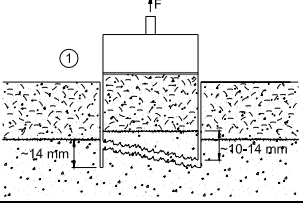
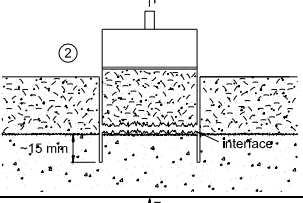
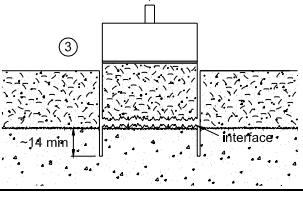
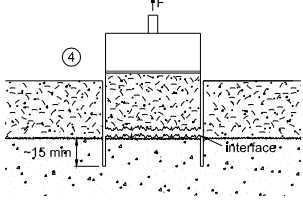
Model	Failure surface sketch	Details of the failure surface
B3C5P2		<p>Failure in the bond-substrate interface, in the bond-overlay interface and in the overlay; Existence of 15 mm de 1 fibra; Existence of voids with $\phi \approx 1.0$ mm.</p>
		<p>Substrate failure; Existence of 5 voids with $\phi \approx 2.5$ mm; Existence of other small voids.</p>
		<p>Overlay failure, and in the bond-substrate interface region; Existence of 2 voids with $\phi \approx 2.5$ mm; Existence of other small voids.</p>
		<p>Failure in the bond-substrate interface; Existence of voids with $\phi \approx 1.0$ mm; Existence of 15 mm of 1 steel fibre;</p>
B3C6P2		<p>Substrate failure; Existence of 4 voids with $\phi \approx 2.5$ mm; Existence of other small voids.</p>
		<p>Failure in the bond-overlay interface region; Existence of 8 mm of 1 steel fibre; Existence of 7 mm of 1 steel fibre; Existence of 4 voids with $\phi \approx 2.0$ mm; Existence of other small voids.</p>
		<p>Failure in the bond-overlay interface region; Existence of 10 mm of 1 steel fibre; Existence of 7 mm of 1 steel fibre; Existence of 4 mm of 1 steel fibre; Existence of 2 voids with $\phi \approx 2.0$ mm;</p>
		<p>Failure in the bond-overlay interface region; Existence of 24 mm of 1 steel fibre; Existence of 13 mm of 1 steel fibre; Existence of 10 mm of 1 steel fibre; Existence of 8 mm of 1 steel fibre; Existence of 5 mm of 1 steel fibre; Existence of 1 void with $\phi \approx 3.0$ mm; Existence of voids with $\phi \approx 1.0$ mm.</p>

Table E9 - Modes and details of failure verified in B3C5P3 and B3C6P3 models.

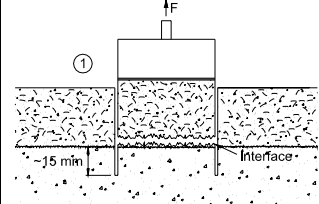
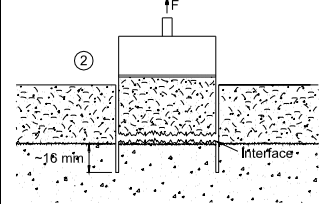
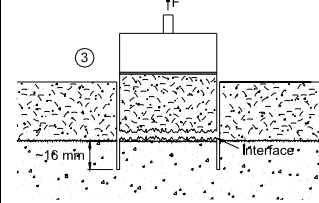
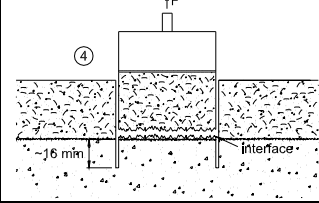
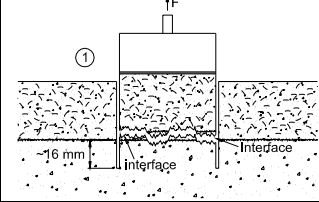
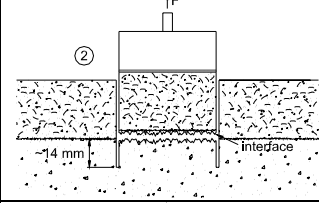
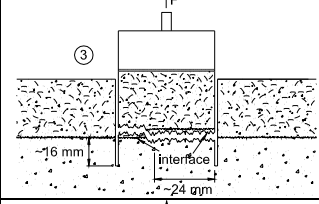
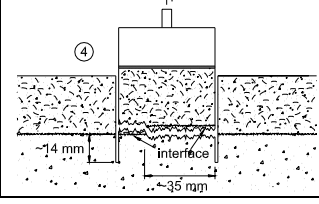
Model	Failure surface sketch	Details of the failure surface
B3C5P3		Failure in the bond-overlay interface; Existence of 4 voids with $\phi \approx 2$ mm.
		Failure in the bond-overlay interface (with paste failure and aggregate-paste bond failure); Existence of voids with $\phi_{\min} \approx 1$ mm and $\phi_{\max} \approx 3$ mm; Existence of other small voids.
		Failure in the bond-overlay interface. Existence of voids with $\phi \approx 1.5$ mm.
		Failure in the bond-overlay interface; Existence of 2 voids with $\phi \approx 2$ mm; Existence of other voids with $\phi \approx 1$ mm.
B3C6P3		Failure in the bond-substrate interface and in the bond-overlay interface; Existence of voids with $\phi \approx 1$ mm.
		Failure in the bond-substrate interface; Existence of a extremity of 1 steel fibre; Existence of 8 mm of 1 steel fibre; Existence of voids with $\phi \approx 1$ mm.
		Failure in the bond-substrate interface and in the bond-overlay interface; Existence of voids with $\phi \approx 1$ mm.
		Failure in the bond-substrate interface and in the bond-overlay interface; Existence of voids with $\phi \approx 1$ mm;

Table E10 - Modes and details of failure verified in B1C1'P3 and B1C2'P3 models.

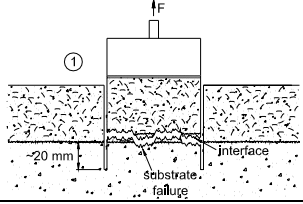
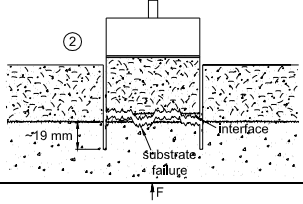
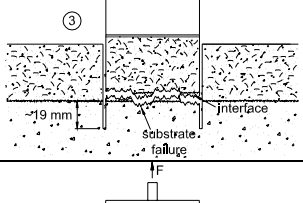
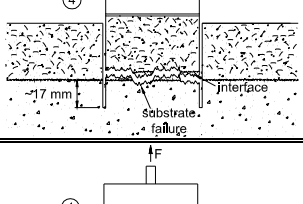
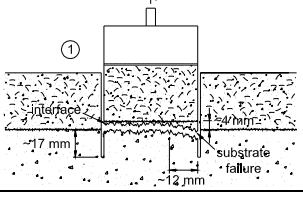
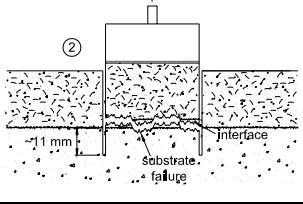
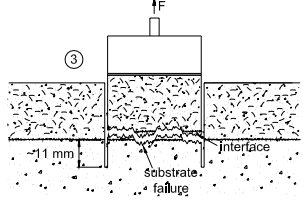
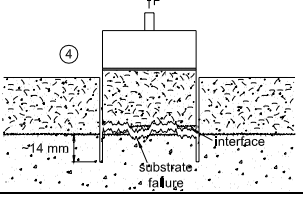
Model	Failure surface sketch	Details of the failure surface
B1C1'P3		<p>Substrate failure just below the bond-substrate interface (combination of paste failure, aggregate failure in 3 aggregates and aggregate-paste bond failure in 2 coarse aggregate), and bond-overlay interface failure (in the high spots part of the substrate surface, i.e. in the stand out part of the coarse aggregates).</p>
		<p>Substrate failure just below the bond-substrate interface (combination of paste failure, aggregate failure in 4 aggregates and aggregate-paste bond failure in 3 coarse aggregate), and bond-overlay interface failure (in the high spots part of the substrate surface, i.e. in the stand out part of the coarse aggregates); Existence of 1 void with $\phi \approx 1$ mm in the substrate;</p>
		<p>Substrate failure just below the bond-substrate interface (combination of paste failure, aggregate failure in 2 aggregates and aggregate-paste bond failure in 3 coarse aggregate), and bond-overlay interface failure (in the high spots part of the substrate surface, i.e. in the stand out part of the coarse aggregates).</p>
		<p>Substrate failure just below the bond-substrate interface (combination of paste failure, aggregate failure in 1 aggregates and aggregate-paste bond failure in 3 coarse aggregate), and bond-overlay interface failure (in the high spots part of the substrate surface, i.e. in the stand out part of the coarse aggregates).</p>
B1C2'P3		<p>Substrate failure just below the bond-substrate interface (combination of paste failure and aggregate-paste bond failure in 3 coarse aggregate), and bond-overlay interface failure (in the high spots part of the substrate surface, i.e. in the stand out part of the coarse aggregates); Existence of 3 voids with $\phi \approx 2$ mm; Existence of other small voids.</p>
		<p>Substrate failure just below the bond-substrate interface (combination of paste failure, aggregate failure in 3 aggregates and aggregate-paste bond failure in 3 coarse aggregate), and bond-overlay interface failure (in the high spots part of the substrate surface, i.e. in the stand out part of the coarse aggregates); Existence of 2 voids with $\phi \approx 1.5$ mm; Existence of other small voids.</p>
		<p>Substrate failure just below the bond-substrate interface (combination of paste failure, aggregate failure in 3 aggregates and aggregate-paste bond failure in 3 coarse aggregate), and bond-overlay interface failure (in the high spots part of the substrate surface, i.e. in the stand out part of the coarse aggregates); Existence of 2 voids with $\phi \approx 2$ mm; Existence of other small voids.</p>
		<p>Substrate failure just below the bond-substrate interface (combination of paste failure, aggregate failure and aggregate-paste bond failure in 3 coarse aggregate), and bond-overlay interface failure (in the high spots part of the substrate surface, i.e. in the stand out part of the coarse aggregates).</p>

Table E11 - Modes and details of failure verified in B2C2'P3 and B2C3'P3 models.

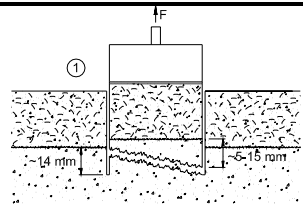
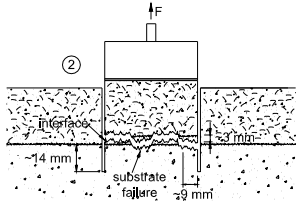
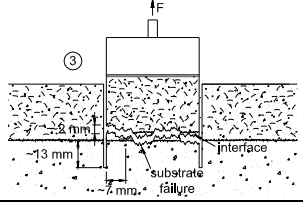
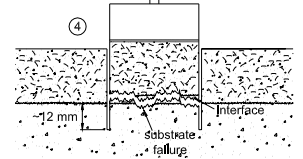
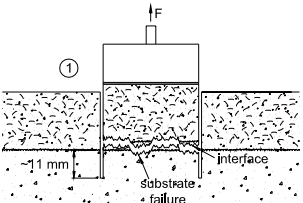
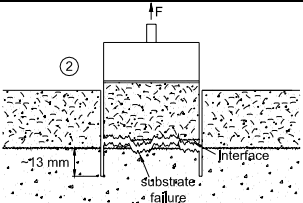
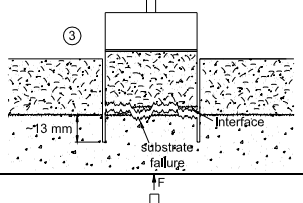
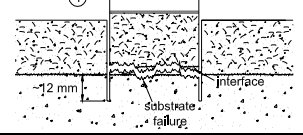
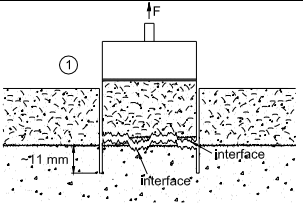
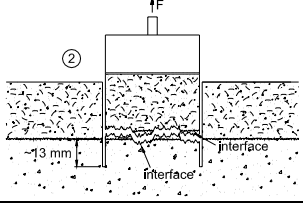
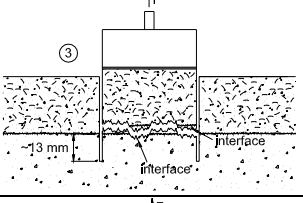
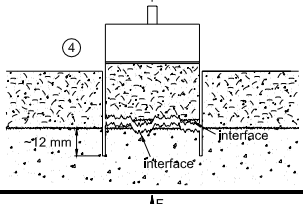
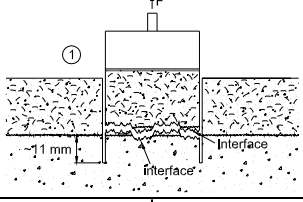
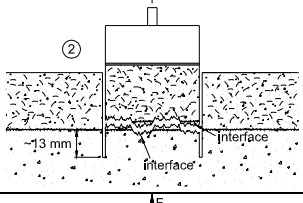
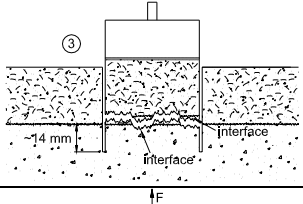
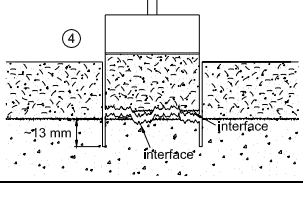
Model	Failure surface sketch	Details of the failure surface
B2C2'P3		<p>Substrate failure: combination of paste failure, coarse aggregate failure in 2 aggregates and aggregate-paste bond failure in 3 coarse aggregates; Existence of 1 void with $\phi \approx 4$ mm; Existence of 1 void with $\phi \approx 1.5$ mm; Existence of others small voids.</p>
		<p>Failure in the bond-overlay interface (located in the high spots part of the substrate surface, i.e. in the stand out part of the coarse aggregates. A uniform bond-line thickness was not kept. Probably the remain water coat of the water used to saturated the surface changed the bond coat thixotropy and the adhesive drained away from the high spots and into the low spots) and failure in the bond substrate interface (levelling to the top substrate surface in the paste and also in the coarse aggregate in 3 aggregates).</p>
		<p>The same failure as in the core test 2. (levelling to the top substrate surface in the paste, in the aggregate-paste interface and also in the coarse aggregate in 2 aggregates) and failure in the overlay (in the aggregate-paste interface of 1 aggregate).</p>
		<p>The same failure as in the core test 2. (levelling to the top substrate surface in the paste, in the coarse aggregate in 2 aggregates and also in the aggregate-paste interface in 1 aggregate).</p>
B2C3'P3		<p>Failure in the bond-overlay interface (located in the high spots part of the substrate surface, i.e. in the stand out part of the coarse aggregates. A uniform bond-line thickness was not kept. Probably the remain water coat of the water used to saturated the surface changed the bond coat thixotropy and the adhesive drained away from the high spots and into the low spots) and failure in the bond-substrate interface (levelling to the top substrate surface in the paste and also in the coarse aggregates).</p>
		<p>The same failure as in the core test 1.</p>
		<p>The same failure as in the core test 1.</p>
		<p>The same failure as in the core test 1.</p>

Table E12 - Modes and details of failure verified in B3C4'P3 and B3C5'P3 models.

Model	Failure surface sketch	Details of the failure surface
B3C4'P3		Bond-substrate interface failure and bond-overlay interface failure (in the high spots part of the substrate surface, i.e. in the stand out part of the coarse aggregates).
		The same failure as in the core test 1.
		The same failure as in the core test 1.
		The same failure as in the core test 1.
B3C5'P3		Bond-substrate interface failure and bond-overlay interface failure (in the high spots part of the substrate surface, i.e. in the stand out part of the coarse aggregates).
		The same failure as in the core test 1.
		The same failure as in the core test 1.
		The same failure as in the core test 1.

Annex F - Data of the tests for two controlled stress rates

Table F1 - Results of the pull-off tests for different stress rates in series of C20/30 strength class of the concrete base.

Model	Stress rate (MPa/s)	Concrete age (days)		f _c (at 28 days in MPa)		Test	F _{PRÉ} (kN)	F (kN)	F _{TOT} (kN)	S _{PO} (MPa)	S _{PO,m} (MPa)	Std. dev. (MPa)	COV. (%)
		Base	Layer	Base	Layer								
B1C1	0.05 ^(*)	66	31	22.32	25.87	1	-	-	2.680	1.48	1.58	0.18	11.32
						2	-	-	3.310	1.83			
						3	-	-	2.850	1.57			
						4	-	-	2.580	1.43			
	0.02	442	407			1	0.32	2.65	2.971	1.76	1.73	0.14	7.97
						2	0.26	2.28	2.530	1.50			
						3	0.28	2.68	2.959	1.76			
						4	0.22	2.95	3.161	1.88			
						5	0.35	2.62	2.967	1.76			
	0.15	442	407			1	0.30	1.83	2.122	1.26	1.68	0.34	20.13
						2	0.18	3.25	3.436	2.04			
						3	0.32	2.39	2.715	1.61			
4				0.23	3.19	3.413	2.02						
5				0.15	2.42	2.563	1.52						
6				0.27	2.15	2.416	1.43						
7				0.25	3.38	3.621	2.15						
8				0.36	2.04	2.394	1.42						
B1C2	0.05 ^(*)	67	32	22.32	32.08	1	-	-	2.700	1.49	1.83	0.28	15.13
						2	-	-	3.330	1.84			
						3	-	-	3.930	2.17			
						4	-	-	3.320	1.83			
	0.02	443	408			1	0.30	2.81	3.104	1.84	1.73	0.09	5.32
						2	0.17	2.87	3.036	1.80			
						3	0.26	2.65	2.916	1.73			
						4	0.23	2.57	2.799	1.66			
						5	0.22	2.52	2.734	1.62			
	0.15	443	408			1	0.18	3.19	3.365	2.00	1.99	0.42	20.99
						2	0.21	2.40	2.606	1.55			
						3	0.24	3.28	3.518	2.09			
						4	0.32	3.59	3.908	2.32			
						5	0.26	4.03	4.284	2.54			
						6	0.21	2.29	2.497	1.48			

Note: Coefficient of Variation (COV) = (Standard deviation/Average) x 100

^(*) approximately, carried out manually with Proceq DYNA Z15

Table F2 - Results of the pull-off tests for different stress rates in series of C40/50 strength class of the concrete base.

Model	Stress rate (MPa/s)	Concrete age (days)		f _c (at 28 days in MPa)		Test	F _{PRÉ} (kN)	F (kN)	F _{TOT} (kN)	S _{PO} (MPa)	S _{PO,m} (MPa)	Std. dev. (MPa)	COV. (%)
		Base	Layer	Base	Layer								
B2C3	0.05 ^(*)	71	32	42.59	41.5	1	-	-	4.520	2.50	2.59	0.17	6.68
						2	-	-	4.980	2.75			
						3	-	-	4.320	2.39			
						4	-	-	4.900	2.71			
	0.02	428	389			1	0.32	3.80	4.125	2.59	2.79	0.25	9.04
						2	0.30	3.72	4.013	2.52			
						3	0.28	4.37	4.652	2.92			
						4	0.28	4.66	4.933	3.10			
						5	0.24	3.85	4.090	2.57			
						6	0.24	4.53	4.773	3.00			
	0.15					1	0.30	4.22	4.511	2.84	3.08	0.33	10.71
						2	0.29	4.89	5.183	3.26			
						3	0.28	3.95	4.232	2.66			
						4	0.21	4.80	5.009	3.15			
						5	0.28	5.26	5.540	3.48			
B2C4	0.05 ^(*)	73	36	42.59	53.51	1	-	-	4.530	2.50	2.35	0.28	11.83
						2	-	-	4.780	2.64			
						3	-	-	3.650	2.02			
						4	-	-	4.050	2.24			
	0.02					1	0.29	3.248	3.538	2.10	2.06	0.07	3.48
						2	0.27	3.26	3.530	2.09			
						3	0.25	3.04	3.287	1.95			
						4	0.35	3.17	3.515	2.09			
	0.15	418	379			1	0.22	3.06	3.282	1.95	2.12	0.30	14.04
						2	0.25	2.88	3.134	1.86			
						3	0.28	3.73	4.005	2.38			
						4	0.29	2.91	3.200	1.90			
						5	0.29	4.09	4.382	2.60			
						6	0.23	3.25	3.485	2.07			

Note: Coefficient of Variation (COV) = (Standard deviation/Average) x 100

^(*) approximately, carried out manually with Proceq DYNA Z15

Table F3 - Results of the pull-off tests for different stress rates in series of C60/750 strength class of the concrete base.

Model	Stress rate (MPa/s)	Concrete age (days)		f _c (at 28 days in MPa)		Test	F _{PRÉ} (kN)	F (kN)	F _{TOT} (kN)	S _{PO} (MPa)	S _{PO,m} (MPa)	Std. dev. (MPa)	COV. (%)
		Base	Layer	Base	Layer								
B3C5	0.05 ^(*)	72	35	60.82	62.54	1	-	-	8.300	4.59	4.20	0.27	6.47
						2	-	-	7.150	3.95			
						3	-	-	7.430	4.11			
						4	-	-	7.530	4.16			
	0.02	435	398			1	0.24	4.09	4.338	2.57	2.91	0.23	8.03
						2	0.22	4.36	4.582	2.72			
						3	0.31	4.62	4.930	2.92			
						4	0.25	5.00	5.242	3.11			
						5	0.23	4.68	4.913	2.91			
						6	0.34	5.05	5.389	3.20			
	0.15	435	398			1	0.27	4.71	4.981	2.95	3.44	0.30	8.76
						2	0.25	6.05	6.307	3.74			
3				0.32	6.03	6.341	3.76						
4				0.29	5.28	5.569	3.30						
5				0.20	5.18	5.380	3.19						
6				0.27	5.83	6.094	3.61						
7				0.25	5.66	5.910	3.51						
8				0.25	5.66	5.910	3.51						
B3C6	0.05 ^(*)	72	35	60.82	66.81	1	-	-	7.020	3.88	3.73	0.29	7.70
						2	-	-	6.730	3.72			
						3	-	-	6.020	3.33			
						4	-	-	7.200	3.98			
	0.02	439	402			1	0.30	4.05	4.358	2.59	3.25	0.48	14.93
						2	0.30	5.84	6.146	3.65			
						3	0.29	5.62	5.901	3.50			
						4	0.31	5.80	6.113	3.63			
						5	0.22	4.64	4.855	2.88			
	0.15	439	402			1	0.24	3.75	3.989	2.37	2.81	0.36	12.92
						2	0.32	5.28	5.594	3.32			
						3	0.27	4.99	5.263	3.12			
4				0.25	3.95	4.196	2.49						
5				0.16	4.48	4.640	2.75						
6				0.28	4.47	4.742	2.81						

Note: Coefficient of Variation (COV) = (Standard deviation/Average) x 100

^(*) approximately, carried out manually with Proceq DYNA Z15